Schweizerische Eidgenossenschaft
Confédération suisse
Confederazione Svizzera
Confederaziun svizra

Federal Department of the Environment,
Transport, Energy and Communications DETEC

Swiss Federal Office of Energy
Energy Research and Cleantech

Final report from 12 December 2025

Delight

Design and Evaluation of Lightweight Composite PV Modules for Integration in Buildings and Infrastructure

Publisher:
Swiss Federal Office of Energy SFOE
Energy Research and Cleantech
CH-3003 Berne
www.energy-research.ch

Subsidy recipients:
EPFL
Rue de la Maladière 71 B
CH-2002 Neuchatel
www.epfl.ch

Autors:
Umang Desai, EPFL, umang.desai@epfl.ch
Antonin Faes, EPFL, antonin.faes@epfl.ch
Christophe Ballif, EPFL, christophe.ballif@epfl.ch

SFOE project coordinators:
Stefan Oberholzer, stefan.oberholzer@bfe.admin.ch

SFOE contract number: SI/502501

Summary

Achieving the ambitious targets of decarbonizing the European economy requires a huge effort. Integration of photovoltaic modules on to existing infrastructure is one of the main pillars to reach the targets for renewable electricity, especially for countries where there is not enough free land to build largescale PV plants: either because they are densely populated (Netherlands, Belgium) or mountainous (Austria, Switzerland). Doing this successfully requires simultaneous optimization of energy yield and cost, but also module weight, aesthetics, circularity, reliability, and safety. DELIGHT project brings together expertise in all these areas and will develop highly attractive, and unique solutions for the integration of PV, to enable energy-positive buildings. The following are the main achievements of the DELIGHT project:

1. Validated a reliable, ultra-lightweight material stack (<6 kg/m²): the consortium successfully developed a glass-free module architecture weighing less than 6 kg/m²—less than half the weight of standard glass-glass modules. Through iterative testing, consortium established a specific, qualified Bill of Materials (BoM) that ensures durability: a PET-based frontsheet, POE encapsulant, and a polypropylene (PP) honeycomb composite backsheet. This combination solves the historical issue of polymer fragility, passing critical IEC 61215 reliability standards (damp heat, UV, mechanical load, hail) with less than 5% power degradation.

2. Bridged the gap between aesthetics and performance: The project advanced BIPV by integrating colored polymeric foils (Solaxess) directly into the lightweight stack. It is demonstrated that these modules maintain structural integrity and electrical yield under real-world conditions. This was validated through a demonstration façade in Neuchâtel, Switzerland, where modules have operated for over 9 months with minimal degradation (~1.3%), proving the feasibility of attractive, energy-positive building skins.

3. Defined safety boundaries and future optimization: this work assessed the novel modules for safety protocols to check the compliance related to BIPV products. While the composite modules achieved ISO Class E fire spread criteria suitable for low-rise buildings (<11m), the testing identified "flaming droplets" as the remaining critical challenge. This result provides a clear roadmap for the industry: future iterations must incorporate fire retardants at the encapsulant or backsheet level to achieve unrestricted building code compliance.

Development of such lightweight and aesthetically pleasing modules will enable better acceptance in the consumer market and also help to reduce the mounting time, planning and costs for the installers.

Zusammenfassung

Die Erreichung der ehrgeizigen Ziele zur Dekarbonisierung der europäischen Wirtschaft erfordert enorme Anstrengungen. Die Integration von Photovoltaikmodulen in die bestehende Infrastruktur ist eine der wichtigsten Säulen, um die Ziele für erneuerbaren Strom zu erreichen, insbesondere in Ländern, in denen nicht genügend freie Fläche für den Bau großer PV-Anlagen zur Verfügung steht: entweder aufgrund hoher Bevölkerungsdichte (Niederlande, Belgien) oder aufgrund der Topografie (Österreich, Schweiz). Für den Erfolg sind die gleichzeitige Optimierung von Energieertrag und Kosten, aber auch von Modulgewicht, Ästhetik, Kreislaufwirtschaft, Zuverlässigkeit und Sicherheit erforderlich. Das DELIGHT-Projekt bündelt die Expertise in all diesen Bereichen und entwickelt hochattraktive und einzigartige Lösungen für die PV-Integration, um energiepositive Gebäude zu ermöglichen. Die wichtigsten Ergebnisse des DELIGHT-Projekts sind:

1. Validierung eines zuverlässigen, ultraleichten Materialverbunds (<6 kg/m²): Das Konsortium entwickelte erfolgreich eine glasfreie Modularchitektur mit einem Gewicht von weniger als 6 kg/m² – weniger als die Hälfte des Gewichts von Standard-Glas-Glas-Modulen. Durch iterative Tests etablierte das Konsortium eine spezifische, qualifizierte Stückliste (BoM), die Langlebigkeit gewährleistet: eine PET-basierte Frontfolie, ein POE-Verkapselungsmaterial und eine Rückseitenfolie aus Polypropylen-Wabenverbundwerkstoff (PP). Diese Kombination löst das bisherige Problem der Polymerbrüchigkeit und erfüllt die kritischen Zuverlässigkeitsstandards der IEC 61215 (Feuchte-Wärme-Test, UV-Bestrahlung, mechanische Belastung, Hagel) mit einer Leistungsdegradation von weniger als 5 %.

2. Überbrückung der Kluft zwischen Ästhetik und Leistung: Das Projekt verbesserte die gebäudeintegrierte Photovoltaik (BIPV) durch die Integration farbiger Polymerfolien (Solaxess) direkt in den leichten Materialverbund. Es wurde gezeigt, dass diese Module ihre strukturelle Integrität und ihren elektrischen Ertrag unter realen Bedingungen beibehalten. Dies wurde anhand einer Demonstrationsfassade in Neuchâtel, Schweiz, validiert, wo die Module über 9 Monate mit minimaler Degradation (~1,3 %) betrieben wurden, was die Machbarkeit attraktiver, energiepositiver Gebäudehüllen beweist.

3. Definition von Sicherheitsgrenzen und zukünftiger Optimierung: In dieser Arbeit wurden die neuartigen Module hinsichtlich der Sicherheitsprotokolle bewertet, um die Konformität mit den Anforderungen an BIPV-Produkte zu überprüfen. Obwohl die Verbundmodule die Brandverhaltensklasse E nach ISO für niedrige Gebäude (<11 m) erreichten, identifizierten die Tests „brennende Tropfen“ als die verbleibende kritische Herausforderung. Dieses Ergebnis liefert einen klaren Fahrplan für die Branche: Zukünftige Versionen müssen Flammschutzmittel im Verkapselungsmaterial oder in der Rückseitenfolie enthalten, um die uneingeschränkte Einhaltung der Bauvorschriften zu gewährleisten.

Die Entwicklung solch leichter und ästhetisch ansprechender Module wird zu einer besseren Akzeptanz auf dem Verbrauchermarkt führen und gleichzeitig dazu beitragen, die Montagezeit, die Planung und die Kosten für die Installateure zu reduzieren.

Résumé

Atteindre les objectifs ambitieux de décarbonation de l'économie européenne exige un effort considérable. L'intégration de modules photovoltaïques sur les infrastructures existantes est l'un des principaux piliers pour atteindre les objectifs en matière d'électricité renouvelable, notamment pour les pays où les terrains disponibles sont insuffisants pour la construction de centrales photovoltaïques à grande échelle : soit en raison de leur forte densité de population (Pays-Bas, Belgique), soit de leur relief montagneux (Autriche, Suisse). Pour y parvenir, il est nécessaire d'optimiser simultanément le rendement énergétique et les coûts, mais aussi le poids des modules, leur esthétique, leur circularité, leur fiabilité et leur sécurité. Le projet DELIGHT rassemble des expertises dans tous ces domaines et développera des solutions uniques et très attractives pour l'intégration du photovoltaïque, permettant ainsi la construction de bâtiments à énergie positive. Voici les principales réalisations du projet DELIGHT :

1. Validation d'une structure de matériaux fiable et ultralégère (<6 kg/m²) : le consortium a développé avec succès une architecture de module sans verre pesant moins de 6 kg/m², soit moins de la moitié du poids des modules verre-verre standard. Grâce à des tests itératifs, le consortium a établi une nomenclature (BoM) spécifique et qualifiée garantissant la durabilité : une feuille frontale à base de PET, un encapsulant POE et une feuille arrière composite en nid d'abeille de polypropylène (PP). Cette combinaison résout le problème historique de la fragilité des polymères, en respectant les normes de fiabilité critiques IEC 61215 (chaleur humide, UV, charge mécanique, grêle) avec une dégradation de puissance inférieure à 5 %.

2. Conciliation de l'esthétique et des performances : le projet a fait progresser le BIPV (photovoltaïque intégré au bâtiment) en intégrant des films polymères colorés (Solaxess) directement dans la structure légère. Il a été démontré que ces modules conservent leur intégrité structurelle et leur rendement électrique dans des conditions réelles. Cela a été validé par une façade de démonstration à Neuchâtel, en Suisse, où les modules fonctionnent depuis plus de 9 mois avec une dégradation minimale (~1,3 %), prouvant la faisabilité de revêtements de bâtiments esthétiques et à énergie positive.

3. Définition des limites de sécurité et des optimisations futures : ces travaux ont évalué les nouveaux modules selon les protocoles de sécurité afin de vérifier leur conformité aux produits BIPV. Si les modules composites ont satisfait aux critères de propagation du feu de classe E de la norme ISO, adaptés aux bâtiments de faible hauteur (<11 m), les tests ont identifié les « gouttelettes enflammées » comme le principal défi restant. Ce résultat fournit une feuille de route claire pour l'industrie : les futures versions devront intégrer des retardateurs de flamme au niveau de l'encapsulant ou de la feuille arrière pour une conformité totale aux codes du bâtiment.

Le développement de modules aussi légers et esthétiques permettra une meilleure acceptation sur le marché grand public et contribuera également à réduire le temps de montage, la planification et les coûts pour les installateurs.

Contents

Summary ... 3
Zusammenfassung ... 3
Résumé ... 4
Contents ... 5
List of figures ... 6
List of tables ... 8
List of abbreviations ... 9
1 Introduction ... 10
1.1. Context and motivation ... 10
1.2. Project objectives ... 11
1.3. State-of-the-art ... 12
2 Approach, method, results and discussion ... 13
2.1. Initial prototypes ... 13
2.1.1. Effect of thermal cycling ... 17
2.1.2. Effect of damp-heat ageing ... 18
2.1.3. Effect of humidity freeze ... 19
2.1.4. Effect of hail stones ... 20
2.1.5. Adhesion testing ... 23
2.2. Change in the bill-of-materials for further testing in the form of mini-modules ... 26
2.2.1. Reliability testing of mini-modules against climatic stressors ... 28
2.2.2. Flexural tests ... 30
2.2.3. Static mechanical load tests on mini-modules ... 32
2.2.4. Flammability tests on mini-modules ... 34
2.3. Reliability testing on modules of larger format: effect of sequential ageing ... 35
2.4. Development of novel coatings for frontsheet and its reliability testing ... 38
2.4.1. Reliability testing on the free-standing frontsheets with coatings ... 38
2.4.2. Reliability testing of minimodules containing frontsheets coated with novel coatings ... 40
2.5. Design and fabrication of large sized LW modules for demonstration site at microcity, Neuchatel, Switzerland ... 44
2.6. Development of frameless module design with thin front glass and transparent backsheet at Kalyon PV, Turkey ... 52
2.6.1. Bill of materials ... 52
3 Conclusions and outlook ... 60
4 Publications and other communications ... 62

List of figures

Fig. 1 Example of lightweight BIPV solution for agricultural, commercial, industrial roofs where standard PV solutions are not adapted due to weight limitations. Source: Solarge 11
Fig. 2: Schematic representation of the honeycomb-skin sandwich and the lay-up of different layers for modules 14
Fig. 3 Front view of the modules: PPGF6 structures with (a) M2 size 5BB cells & (b) M10 size 10BB cells; PPGF8 structures with (c) M2 size 5BB cells & (d) M10 size 10BB cells; PETGF structures with (e) M2 size 5BB cells & (f) M10 size 10BB cells; BOPET structure 15
Fig. 4: Selection of testing sequences from IEC 61215-2 standard 17
Fig. 5: Degradation in fill factor for different modules during thermal cycling 18
Fig. 6: (a) EL of 10BB_BOPET sample before (top) and after (bottom) 200 TC and (b) EL of 5BB_BOPET sample before (top) and after (bottom) 200 TC indicating degradation at the edges of the cells. 18
Fig. 7: Degradation in fill factor for different modules during damp-heat ageing 19
Fig. 8: EL images for PETGF based modules before and after DH ageing 19
Fig. 9: Degradation in fill factor for different modules during humidity freeze cycling 20
Fig. 10: EL images for PETGF based modules before and after HF cycling 20
Fig. 11: Visual cues of damage on the modules due to hail-stones: (a) PPGF6, (b) PPGF8, (c) PETGF and (d) BOPET. 21
Fig. 12: EL images of the modules after the hail test: PPGF6 structures with (a) M2 size 5BB cells & (b) M10 size 10BB cells; PPGF8 structures with (c) M2 size 5BB cells & (d) M10 size 10BB cells; PETGF structures with (e) M2 size 5BB cells & (f) M10 size 10BB; BOPET structures with (g) M2 size 5BB cells & (h) M10 size 10BB; Reference module based on glass-glass with (i) M2 size 5BB cells & (j) M10 size 10BB 22
Fig. 13: (a) set-up for 90° peel tests and (b) characteristic load vs displacement diagram. 24
Fig. 14: Effect of 300 hours of DH ageing on the adhesion strength of encapsulant with various skins 24
Fig. 15 Structure of the lightweight PV module based on polymeric honeycomb 27
Fig. 16 Mini-modules based on PPGF8 skins with (a) no coloured, (b) dark grey coloured, and (c) beige coloured foils; as well as based on PPGF6 skins with (d) no coloured, (e) dark grey coloured, and (f) beige coloured foils 28
Fig. 17 (a): Change in relative max. power output with DH ageing, (b): Evolution of IV characteristics with DH ageing for White-transparent sample and (c) Evolution of IV characteristics with DH ageing for black-transparent sample 29
Fig. 18 Evolution of % relative maximum power output with respect to (a) Humidity freeze cycles, (b) thermal cycles and (c) UV dose 30
Fig. 19 (a) The set-up used for four-point bending and (b) indication of two mutually perpendicular directions, longitudinal (L) and transverse (T) of the honeycomb along which the testing is done 31
Fig. 20 Comparison of flexural bending behaviour for PPGF6 and PPGF8 samples along both longitudinal as well as transverse direction 31
Fig. 21 LW modules based on (a) PPGF8 and (b) PPGF6, under static mechanical loading, (c) attachment of a spring-loaded displacement sensor at the back of a module's centre. To keep track of any possible circuit disconnection, the modules were subjected to 1 A current. 32
Fig. 22 EL images of mini-modules for (a) PPGF8 and (b) PPGF6 in the pristine condition & after applying type 1 loading cycles on (d) PPGF8 and (e) PPGF6. Furthermore, EL images of mini-modules consisting PPGF8 (a) before and (f) after applying type 2 loading cycles 33
Fig. 23 Evolution of pressure and displacement profiles with time for the mini modules subjected to type 1 loading based on (a) PPGF8 type backsheet and (b) PPGF6 type backsheet; and type 2 loading on PPGF8 based backsheet for amplitude of (c) 5400 Pa and (d) 8000 33
Fig. 24 Flammability tests for PPGF8 based backsheets (a) before the test and (b) at the instance when the flame propagation is the highest; and for PPGF6 based backsheets (a) before the test and (b) at the instance when the flame propagation is the highest 34

Fig. 25 Visual appearance of the mini-PV modules based on PPGF6 are shown in (a, b and c); while the same is indicated in for PPGF8 in (d, e, and f). 35
Fig. 26: The three sequences used for studying the effect of combination of various climatic stressors 35
Fig. 27: EL images of the module subjected to sequence 1 in (a) pristine condition, (b) after UV exposure, (c) after mechanical loading, (d) after thermal cycling, (e) after humidity freeze cycling; for module subjected to sequence 2 in (f) pristine condition, (g) after DH, (h) after mechanical loading, (i) after humidity freeze cycling, (j) after thermal cycling; and for module subjected to sequence 3 in (k) pristine condition, (l) after DH ageing and (m) after hail impact test 36
Fig. 28: IV curves for modules subjected to sequence 1 (a), sequence 2 (b) and sequence 3 (c). 37
Fig. 29: Light microscopic images; cross-cut for samples after coating application 39
Fig. 30: Transmission curves of the pure PET foil (F0), the coated samples F1 - F4 and - for comparison - the reference samples R (PET+ ETFE) 39
Fig. 31: WVTR of the uncoated PET sample F0 and the coated samples F1-F4 40
Fig. 32: EL images of minimodules in the pristine condition for sample ID (a) R, (b) F0, (c) F1, (d) F2, (e) F3, (f) F4 and after UV ageing for sample ID (g) R, (h) F0, (i) F1, (j) F2, (k) F3, (l) F4. The sample ID are identified in Table 8. 41
Fig. 33: EL images of minimodules in the pristine condition for sample ID (a) R, (b) F0, (c) F1, (d) F2, (e) F3, (f) F4 and after DH ageing for sample ID (g) R, (h) F0, (i) F1, (j) F2, (k) F3, (l) F4. The sample ID are identified in Table 8. 42
Fig. 34 Design of an upscaled module consisting of 40 series connected cells 45
Fig. 35 Upscaled modules based on both PPGF8 and PPGF6 skins. The modules with beige and dark grey coloured foils are based on PPGF6 skins. 45
Fig. 36 EL images for modules based on (a) PPGF8 without coloured foil, (b) PPGF6 without coloured foil, (c) PPGF6 with dark grey coloured foil, and (d) PPGF6 with beige coloured foil. 46
Fig. 37 IV characteristics for upscaled modules 47
Fig. 38 Demonstrator site on microcity rooftop at Neuchatel, Switzerland 48
Fig. 39: Irradiance and max power output profiles for the modules mounted in the form of East facing facade 49
Fig. 40: Power output profile over several days during summer months 50
Fig. 41: EL images for modules mounted in the form of façade: PPGF6-Beige (a) in pristine condition, (b) after 3 months outdoor exposure, (c) after 9 months outdoor exposure; PPGF6-White (d) in pristine condition, (e) after 3 months outdoor exposure, (f) after 9 months outdoor exposure; PPGF6 (g) in pristine condition, (h) after 3 months outdoor exposure, (i) after 9 months outdoor exposure; PPGF8 (j) in pristine condition, (k) after 3 months outdoor exposure, (l) after 9 months outdoor exposure; PPGF8-White (m) in pristine condition, (n) after 3 months outdoor exposure, (o) after 9 months outdoor exposure; PPGF8-Beige (p) in pristine condition, (q) after 3 months outdoor exposure, (r) after 9 months outdoor exposure 51
Fig. 42: Schematic representation of coloured mini modules 53
Fig. 43: Coloured PV mini modules produced at lab scale 54
Fig. 44: I-V graph of coloured mini modules 55
Fig. 45: Coloured modules produced in production scale 56
Fig. 46: Electroluminescence images for Coloured encapsulant based modules: Top: Terracotta; Bottom: Light Green 57
Fig. 47: Real image from the outdoor test center for the one-year I-V characterization monitoring service of the large-scale coloured modules produced. 58
Fig. 48: Electroluminescence images results for coloured encapsulant based module on outdoor test center (left: standard, middle: terra cotta, right: light green) 59
Fig. 49: power output in the STC condition for the three types of modules subjected to outdoor exposure for one year 59

List of tables

Table 1 Current-voltage characteristics of the modules described in Fig. 3 16
Table 2 Weight of the modules described in Fig. 3 16
Table 3 IV characteristics before and after the impact of hail stones 23
Table 4 Other aspects of reliability of skins being studied by other consortium members 25
Table 5: The ranking matrix for various skins being considered 25
Table 6 Results of peel tests carried out for different lamination parameters and encapsulants at the encapsulant-skin interface 26
Table 7: IV characteristics of the modules subjected to sequence 1, 2 and 3 38
Table 8: Samples overview 38
Table 9: IV characteristics before and after the UV ageing for various samples 43
Table 10: IV characteristics before and after the DH ageing for various samples 43
Table 11 Electrical parameters for upscaled modules 47
Table 12: IV characteristics for all the modules installed in the form of facade 52
Table 13: Selected lamination recipe for coloured mini modules 53
Table 14: IV results for coloured mini modules 54
Table 15: Electrical parameters of fabricated PV modules on IV characterization tester in factory 56
Table 16: Electrical parameters of fabricated PV modules on IV characterization tester in outdoor test center 58

List of abbreviations

SFOE	Swiss Federal Office of Energy
PP	Polypropylene
TPO	Thermoplastic polyolefin
PET	Polyethylene terephthalate
IEC	International Electrotechnical Commission
MPP	Maximum power point
BPDs	Bypass diodes
POE	Polyolefin elastomer
HC	Honeycomb
EL	Electroluminescence
Fs	Flame spread
PIB	Polyisobutylene

1 Introduction

1.1. Context and motivation

The European Union (EU) has established ambitious climate and energy targets to achieve by 2030 and a commitment to reach carbon neutrality by 2050. Solar photovoltaic (PV) technology is positioned as a critical driver in meeting these goals, due to its capacity for decentralized, clean energy generation. To support these objectives, PV technology must address three major market requirements: (1) comparable energy yield metrics across various module types, (2) consistent, long-term performance, and (3) a reduced carbon footprint. Ensuring these qualities in PV modules would benefit both private and public sector buyers by enabling informed decisions based on standardized performance and environmental criteria.

A key strategy in this transition involves the integration of PV systems directly into existing infrastructure, including both new and renovated buildings. Building-integrated photovoltaics (BIPV) provides an ideal solution for generating renewable energy in space-constrained urban and industrial areas where installing traditional, land-intensive PV farms is impractical. Densely populated countries like Belgium and the Netherlands, as well as mountainous regions such as Austria and Switzerland, face significant spatial limitations for ground-mounted PV installations. As a result, the integration of PV modules into buildings and infrastructure has become essential to meet renewable energy goals in these regions. For instance, incorporating PV into public buildings and infrastructure can significantly improve energy efficiency and support national energy targets.

However, the current PV market faces a notable barrier: traditional PV modules are often too heavy for widespread adoption in building and infrastructure applications. Many commercial, industrial, and agricultural buildings, comprising up to 40% of building stock in the EU, have structural limitations that prevent the installation of conventional PV panels, which typically weigh over 12 kg/m², or even more with glass/glass designs. This is particularly critical for aging infrastructure, such as older agricultural buildings with asbestos roofs that need replacement, representing approximately 70 km² in the Netherlands alone.

The DELIGHT project brought together leading experts in the field of photovoltaics with collaborators from several European countries like, Austria, Belgium, Türkiye and Switzerland with a common goal to develop a lightweight aesthetically pleasing PV solutions for building integration. Aiming to develop and deploy innovative PV modules that weigh 50% less than traditional modules, DELIGHT seeks to unlock new market potential and make solar power viable for previously unsuitable sites. With a target weight of ≤6 kg/m² for glass-free designs, DELIGHT's solutions open up possibilities for greater integration flexibility across diverse applications, even in areas with limited load-bearing capacity. By pioneering lightweight BIPV technology, the project not only supports EU climate goals but also aligns with ongoing initiatives such as the Building Renovation Wave and the New European Bauhaus, both of which emphasize sustainable, aesthetically integrated, and energy-efficient buildings.

The rise in demand for BIPV aligns with broader environmental and economic incentives within the EU. Lightweight BIPV technology supports the EU's circular economy by promoting PV

solutions with lower embodied carbon, modular integration options, and greater recyclability. With these advancements, DELIGHT's innovations are expected to foster market confidence, encouraging broader PV adoption in both public and private sectors. This approach not only propels Europe toward carbon neutrality but also paves the way for zero-emission, energy-positive buildings and infrastructure that balance functionality, safety, and visual appeal.

1.2. Project objectives

There are several challenges in the BIPV market today. Next to economic aspects and benefits functional integration of solar power systems is key for large-scale application in the built environment. In such a system, primary building envelope functionalities, (e.g., stiffness, wind and water tightness, roof and facade cladding) need to be combined with the generation of solar electricity. Moreover, there is a strong demand for aesthetically pleasing solutions. Meeting all these requirements at the same time is challenging, but when these challenges can be met, there are huge opportunities in the BIPV market.

Fig. 1 Example of lightweight BIPV solution for agricultural, commercial, industrial roofs where standard PV solutions are not adapted due to weight limitations. Source: Solarge

Therefore, the main objective of DELIGHT is to design, manufacture, and evaluate sustainable lightweight composite PV modules for easier integration into existing infrastructure (buildings, transport infrastructure, see Fig. 1) with a special focus on increased safety and optimized aesthetic and constructive integration. The following two design approaches will be tried under this project: a glass-free module design with weight target of ≤ 6 kg/m² (EPFL) and a frameless module design with front glass with a weight target of ≤ 7 kg/m² (Kalyon PV). The three main pillars of the project are:

- Reducing the module weight of the PV-modules and the construction system by development and optimization of innovative lightweight module designs using polymeric frontsheet materials, replacing glass (e.g., composite backsheets using honeycomb structures), with no frames and the use of innovative adhesive or Velcro fastener connection approaches
- Fulfilling the demands for aesthetic integration by introducing colors and specific surface appearance in the PV module stacks (surface coatings, colored encapsulants) while preserving their mechanical, electrical performances and reliability.
- Optimizing the electrical module design in respect to shade-tolerant module topologies with two main goals: (i) improved performance under non-uniform operating conditions

– such as partial shading – and in case of non-uniform module degradation, and (ii) improved safety and reliability (module shut-down; disconnection of damaged sub-strings; reduction or elimination of hot-spots).

An additional cross-sectional objective is to increase the overall sustainability of the light weight modules and its components. Specific targets are the replacement of fluoropolymer frontsheets with solutions based on coated polyester films or the use of recycled PET for the honeycomb structures.

1.3. State-of-the-art

The DELIGHT project focuses on development of rigid, glass-free & aesthetically pleasing PV modules utilizing crystalline silicon solar cell technology for the building integration application. Some of the existing commercially available solutions for lightweight PV module developments are as below:

- **Solarge**[1] has developed a composite solar panel that replaces traditional glass with a lightweight honeycomb material. This design achieves weight savings of up to 65%, resulting in panels that weigh approximately **14.5 kg for a 2.66 m²** module, compared to over 28 kg for conventional glass modules. The honeycomb structure not only reduces weight but also enhances rigidity and impact resistance, making the panels suitable for various applications, including rooftops with weight constraints[2]. Their approach also yields weight reduction **below 6 kg/m²** and gives modules that are mechanically rigid. Solarge modules are designed primarily for rooftop applications, especially where traditional solar panels may be unsuitable due to weight constraints. Their flagship product line, **SOLO**[3], utilizes polymer materials instead of conventional glass and aluminum, resulting in panels that are significantly lighter and easier to handle. **However, such modules are currently only available in white colored backsheets and don't incorporate colored foils, making their technology slightly on backfoot. Furthermore, the DELIGHT project aims to check the feasibility of four different candidate backsheets—one of which weighing as low as 3.3 kg/m², in combination with colored foils—making the modules aesthetically pleasing and at the forefront of the competition for building integration.**
- **DAS Energy** has reduced the weight of their photovoltaic modules by substituting the conventional glass pane with a highly transparent composite material, achieving a weight of just **3.3 kg/m².** This is significantly lower than traditional glass modules, which weigh on average over 20 kg/m². Their patented technology of the modules consists primarily of a proprietary fiberglass-reinforced plastic core (pre-preg), responsible for both flexibility and stability[4]. This design makes modules **semi-flexible,** which not only minimizes weight but also allows the modules to conform to curved surfaces. **However, such a process (pre-preg) may not be suitable for high throughput production since the resin of such a composite material is partially cured, making it tacky**

[1] https://solarge.com/en/
[2] EconCore, Solarge launch lightweight, sustainable solar panel, 14/4/2023, link:https://www.compositesworld.com/news/econcore-solarge-launch-lightweight-sustainable-solar-panel?
[3] https://solarge.com/en/products/solo/
[4] https://das-energy.com/en/technology

requiring extra protecting foils to be applied during storage. The backplane of DE-LIGHT modules does not require such special attention and can be cut into a required size and shape right before the lamination.

- **MET-solar**[5] uses an approach of making flexible modules that uses a highly transparent polymeric foil at front to replace the glass and a polymeric backsheet at back, yielding a PV module that weighs **3 kg/m²**. Such a module is suitable for application such as mobility, marine or custom lighting applications. **However, the mechanical resilience of these modules is under question and thus limits its use to only application areas other than building integration.**

Various other options in market are also available but are mostly based on glass/glass or glass/backsheet-based design making them bulky; hence, excluded from discussion here.

2 Approach, method, results and discussion

2.1. Initial prototypes

Kalyon and IMEC have worked together to implement standard 5BB M2 size (156.75 mm) PERC cells and larger 10 BB M10 size (182 mm) PERC cells to reduce costs. These cells are manufactured in the integrated factory of Kalyon PV in Türkiye.

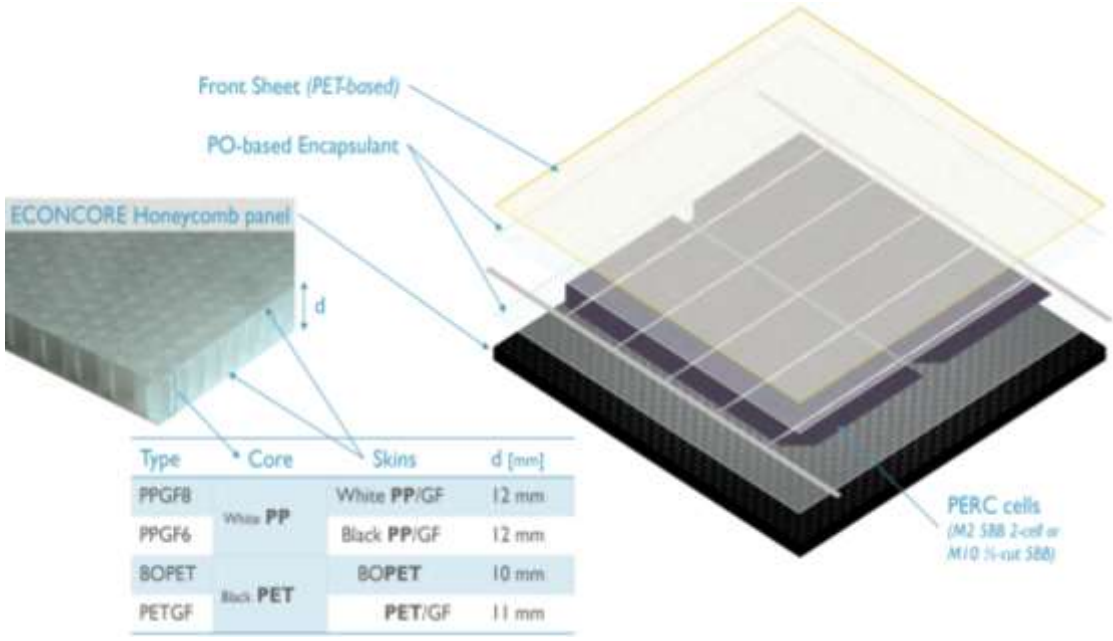

Type	Core	Skins	d [mm]
PPGF8	White PP	White PP/GF	12 mm
PPGF6		Black PP/GF	12 mm
BOPET	Black PET	BOPET	10 mm
PETGF		PET/GF	11 mm

[5] https://metsolar.eu/products/met-flexible/

Fig. 2: Schematic representation of the honeycomb-skin sandwich and the lay-up of different layers for modules

The sandwich structures to be used in the lightweight modules are prepared by thermoplastically adhering the two skins to the honeycomb core by consortium partner Econcore. For this approach, as can be seen in

Fig. 2, PP and PET are chosen as the honeycomb core materials. The white-colored PP core is attached with either white PP skins reinforced with the glass-fibers (hereafter called as PPGF8 structure) or black PP skins reinforced with the glass fibers (hereafter called as PPGF6 structure). Additionally, the black colored PET core is attached either to the bidirectionally oriented PET skins (hereafter called as BOPET structure) or to the glass-fiber reinforced PET skins (hereafter called as PET/GF structure). These sandwich structures are then stacked with the layers of thermoplastic encapsulant, solar cells, thermoplastic encapsulants, and skins, as shown in

Fig. 2. The vacuum lamination was done on the modules at 135°C temperature and 300 mbar membrane pressure. The fabricated modules are depicted in Fig. 3, below. The current-voltage characteristics and weight of the modules are provided in Table 1 and Table 2, respectively.

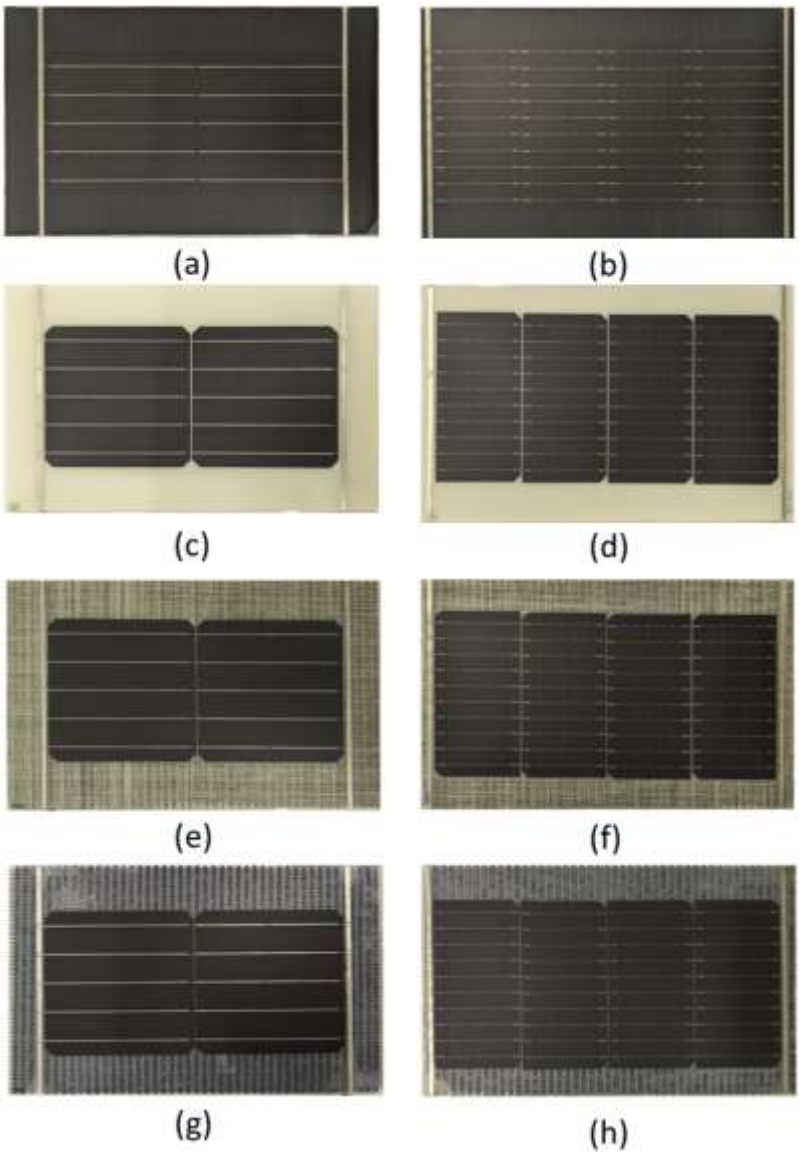

Fig. 3 Front view of the modules: PPGF6 structures with (a) M2 size 5BB cells & (b) M10 size 10BB cells; PPGF8 structures with (c) M2 size 5BB cells & (d) M10 size 10BB cells; PETGF structures with (e) M2 size 5BB cells & (f) M10 size 10BB cells; BOPET structure

Table 1 Current-voltage characteristics of the modules described in Fig. 3

Specimen	I_{sc} [A]	V_{oc} [V]	FF [%]	P_{mpp} [W]
5BB_PPGF6	9.56 ± 0.11	1.34 ± 0.00	78.5 ± 0.2	10.05 ±0.12
10BB_PPGF6	6.51 ± 0.08	2.78 ± 0.01	81.3 ± 0.2	14.70 ± 0.20
5BB_PPGF8	9.91 ± 0.17	1.34 ± 0.01	78.3 ± 0.1	10.41 ± 0.20
10BB_PPGF8	6.74 ± 0.07	2.78 ± 0.01	81.1 ± 0.3	15.22 ± 0.16
5BB_PETGF	9.74 ± 0.12	1.34 ± 0.01	78.0 ± 0.1	10.20 ± 0.19
10BB_PETGF	6.60 ± 0.08	2.78 ± 0.00	81.3 ± 0.4	14.92 ± 0.16
5BB_BOPET	9.66 ± 0.13	1.35 ± 0.00	78.3 ± 0.2	10.18 ± 0.13
10BB_BOPET	6.52 ± 0.08	2.78 ± 0.01	81.7 ± 0.3	14.80 ± 0.16
5BB_GLASS	9.92 ± 0.31	1.34 ± 0.01	78.0 ± 0.4	10.39 ± 0.29

Table 2 Weight of the modules described in Fig. 3

Specimen	Weight [g]	Weight [kg/m^2]
5BB_PPGF6	450	4.5
10BB_PPGF6	456	4.6
5BB_PPGF8	483	4.8
10BB_PPGF8	487	4.9
5BB_PETGF	421	4.2
10BB_PETGF	426	4.3
5BB_BOPET	334	3.3
10BB_BOPET	339	3.4

The developed modules are analysed for further for reliability testing by subjecting them to accelerated ageing against environmental stressors such as damp-heat ageing, thermal cycling and humidity-freeze. The reliability of the modules was also tested against hail-stones and the adhesion at encapsulant-skin interface was also assessed before and after the damp-heat ageing. Furthermore, it was decided to understand first the effect of individual environmental stressors only. At the advanced stages, the consortium has decided to adapt two testing sequences that combine several factors from the IEC 61215-2. Fire safety, wet leakage and effect of hail-impact is considered as critical stressors, in addition to the environmental stressors such as UV radiation, moisture and thermal cycling. The testing sequences, C and E, adapted from the IEC 61215-1 are presented below (Fig. 4):

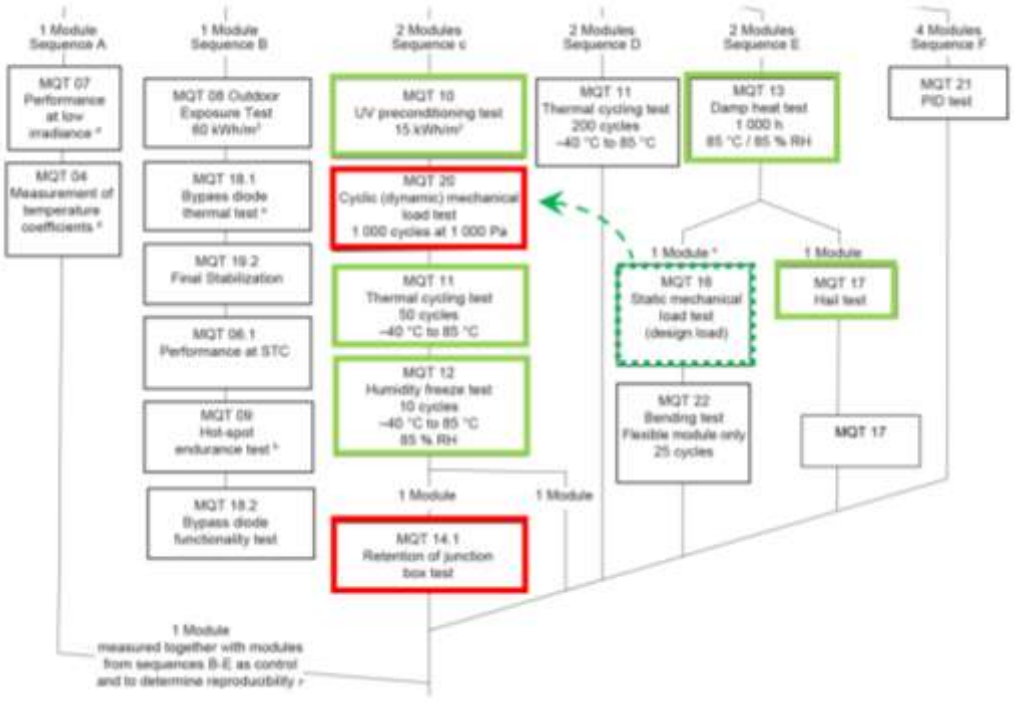

Fig. 4: Selection of testing sequences from IEC 61215-2 standard

2.1.1. Effect of thermal cycling

Fig. 5 indicates the performance degradation during TC in terms of FF. The performance at maximum power point (Pmpp) could also be shown but due to the limited degradation so far (in the range of percentages) this would distort the graphs due to variations in Isc related to the calibration accuracy of the solar simulator (as these are also in the lower %-range). Very limited degradation is observed for all 10BB samples, except for the BOPET samples (an additional one, 10BB_BOPET_5, was made as verification after the first one failed early). This sample showed a significant drop in FF and consequently Pmpp beyond 150 thermal cycles. EL imaging in Fig. 5 indicates that this is due to an interconnect failure. Though it could be that 1 or more wire got fully detached from the cell metallization, it is more likely that 1 or more wires was broken, a failure mode that has been reported earlier (albeit with ribbons instead of wires) [1].

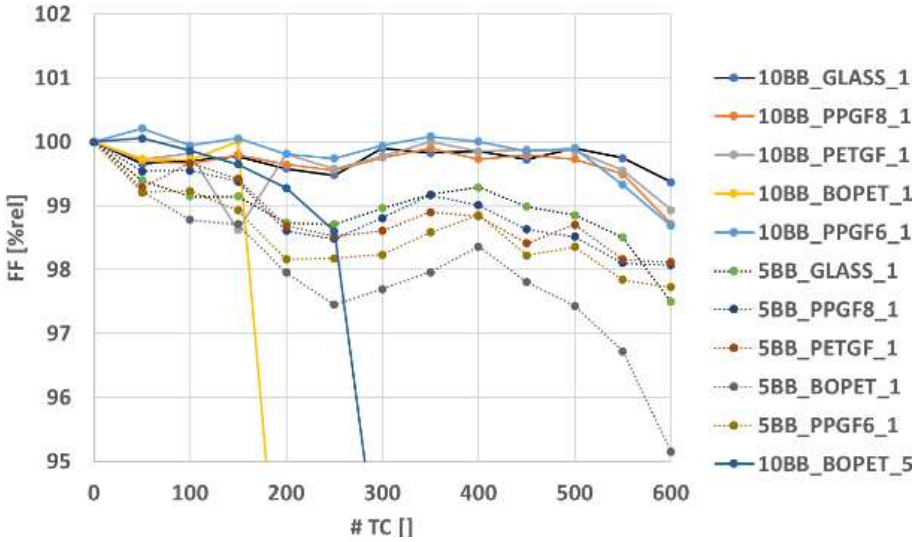

Fig. 5: Degradation in fill factor for different modules during thermal cycling

Fig. 5 also indicates a slight but consistent degradation of all 5BB samples compared to the 10BB ones. This might be attributed to a pressure contact at the edges of the cells, which is formed during lamination but is released in subsequent TC. Fig. 6 shows the EL footprint of this mechanism for the BOPET sample as a reduced intensity at the edges of the cells, which is also observed for all other 5BB samples. Similarly, as for the 10BB laminates, the BOPET version of the 5BB laminates is the first to fail.

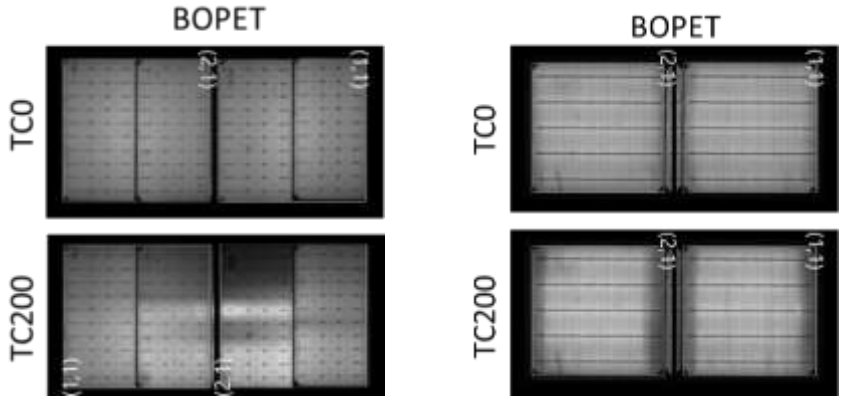

(a) (b)

Fig. 6: (a) EL of 10BB_BOPET sample before (top) and after (bottom) 200 TC and (b) EL of 5BB_BOPET sample before (top) and after (bottom) 200 TC indicating degradation at the edges of the cells.

2.1.2. Effect of damp-heat ageing

During DH testing, for which the results are shown in Fig. 7, no significant degradation is observed except for the 10BB_PETGF sample.

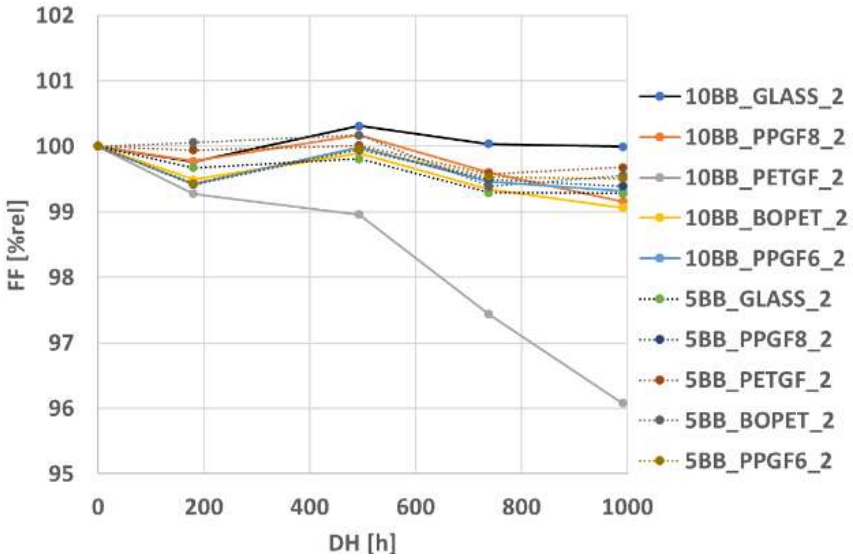

Fig. 7: Degradation in fill factor for different modules during damp-heat ageing

Looking into the EL images before and after DH is shown in Fig. 8, some degradation is observed throughout the different cells in the module. It is clear that the degradation is not specifically coming from the edges, and not all cells are affected equally. Unlike with glass-glass encapsulation, where moisture can only gradually get to the cells from the sides, the lightweight (glass fibre reinforced) polymer encapsulation will be less of a barrier due to the higher WVTRs of the polymers. The edges of the honeycomb are also not fully sealed.

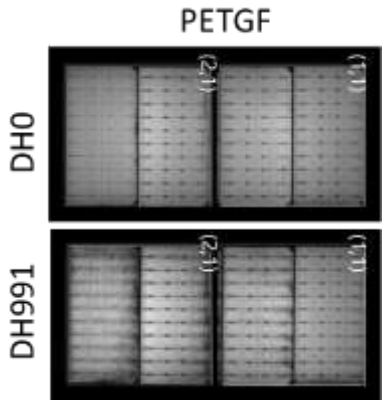

Fig. 8: EL images for PETGF based modules before and after DH ageing

2.1.3. Effect of humidity freeze

HF testing results are given in Fig. 9. With the basic test comprising 10 HF cycles, no significant degradation was observed. However, with extended testing to 20 HF cycles, some degradation appears for the 10BB_PETGF sample and to a lesser extent for the 10BB_BOPET sample.

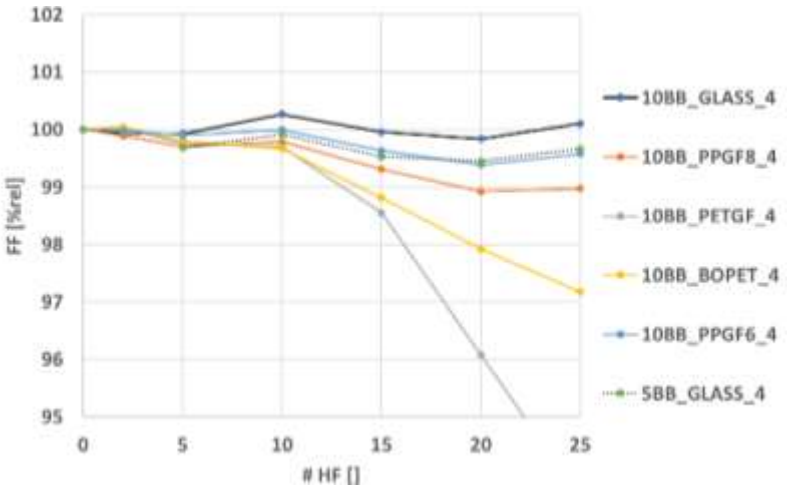

Fig. 9: Degradation in fill factor for different modules during humidity freeze cycling

At first glance, EL imaging after HF (Fig. 10) indicates a similar degradation footprint as for DH (Figure 8).

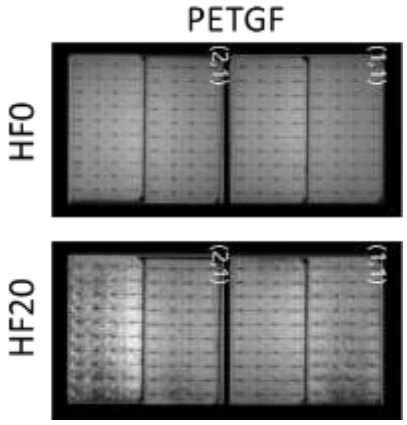

Fig. 10: EL images for PETGF based modules before and after HF cycling

2.1.4. Effect of hail stones

Hail stones of the mass ranging between 6.5-8 g were shot at five different spots on the modules in the range of speed between 21-25m/s, as per the IEC 61215 standard. The modules are then inspected visually (Fig. 11), under the EL images (Fig. 12) and for the IV characteristics (Table 3).

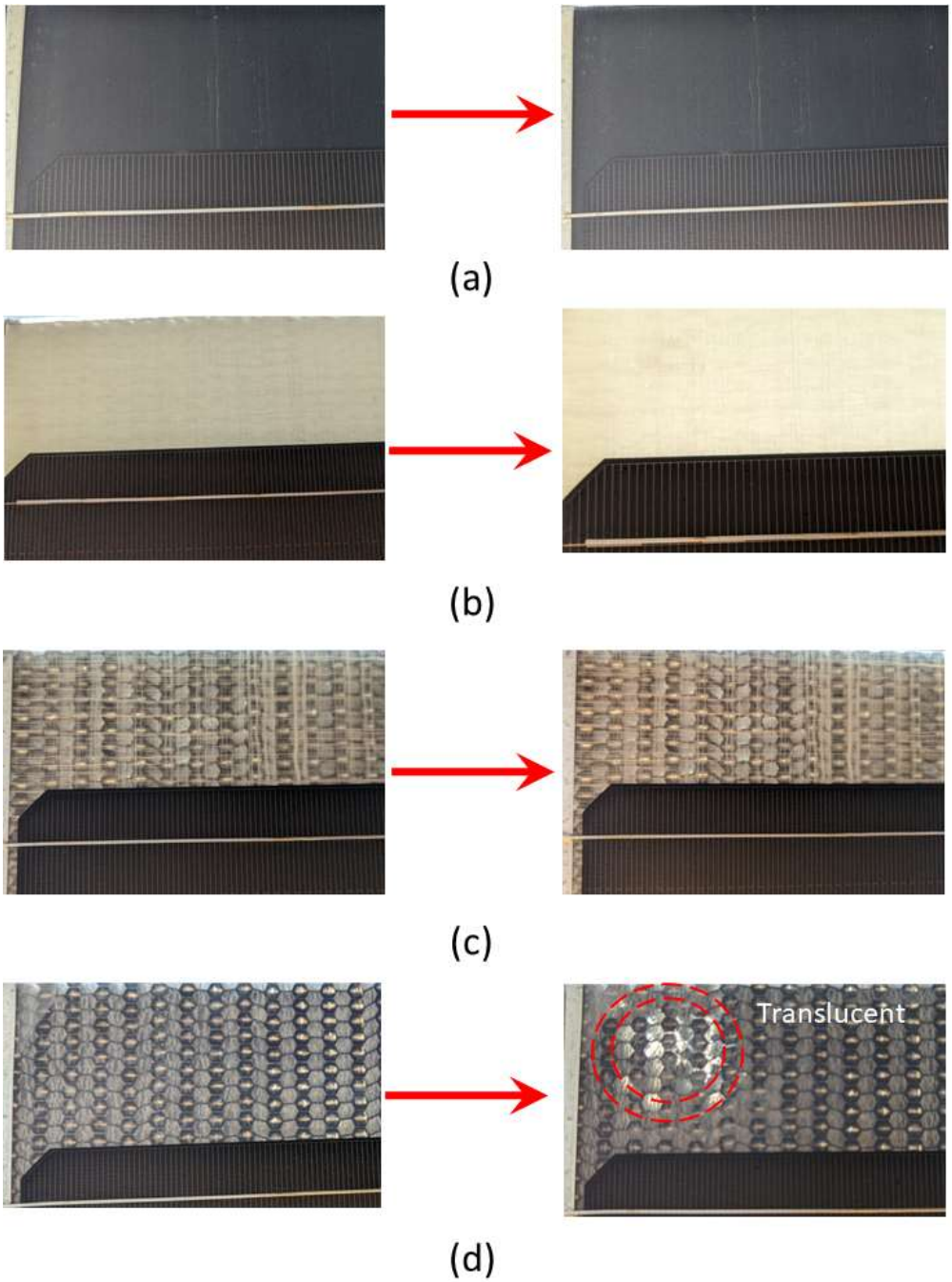

Fig. 11: Visual cues of damage on the modules due to hail-stones: (a) PPGF6, (b) PPGF8, (c) PETGF and (d) BOPET.

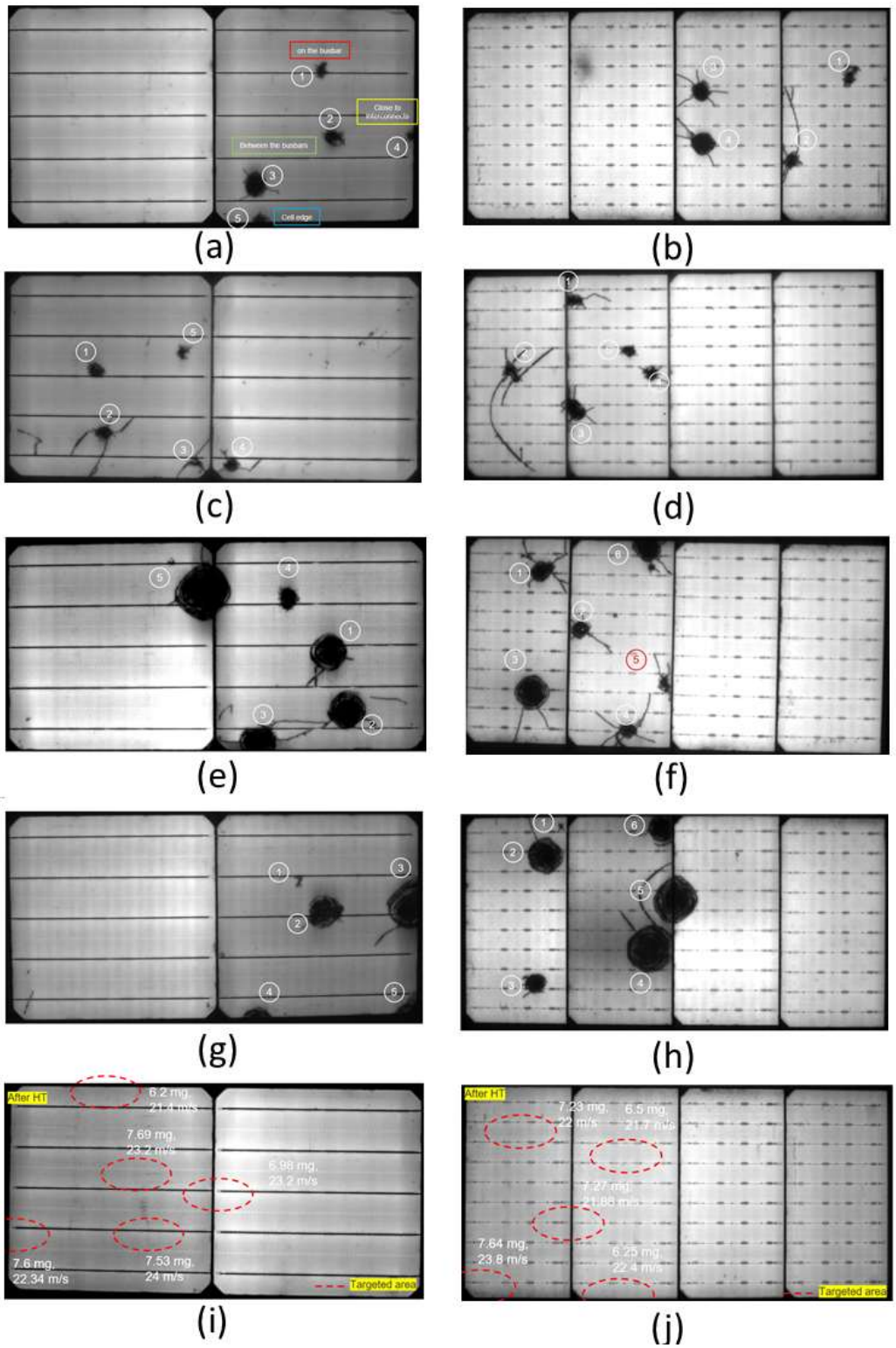

Fig. 12: EL images of the modules after the hail test: PPGF6 structures with (a) M2 size 5BB cells & (b) M10 size 10BB cells; PPGF8 structures with (c) M2 size 5BB cells & (d) M10 size 10BB cells; PETGF structures with (e) M2 size 5BB cells & (f) M10 size 10BB; BOPET structures with (g) M2 size 5BB cells & (h) M10 size 10BB; Reference module based on glass-glass with (i) M2 size 5BB cells & (j) M10 size 10BB

Table 3 IV characteristics before and after the impact of hail stones

Specimen	Condition	Isc (mA)	Voc (V)	FF (%)	P_{max} (W)	% change in P_{max}
5BB_PPGF6	Pristine	8918.42	1.31	77.4	9.042	-
	After hail test	8901.69	1.31	74.7	8.692	-3.87
10BB_PPGF6	Pristine	6177.25	2.738	79.3	13.409	-
	After hail test	6104.93	2.724	76	12.6	-6.03
5BB_PPGF8	Pristine	9359.49	1.32	76.8	9.479	-
	After hail test	9253.91	1.315	75.3	9.165	-3.31
10BB_PPGF8	Pristine	6447.38	2.743	79.5	14.058	-
	After hail test	6411.45	2.733	74.9	13.1	-6.81
5BB_PETGF	Pristine	9108.54	1.323	76.6	9.235	-
	After hail test	8996.37	1.296	68.2	7.956	-13.84
10BB_PETGF	Pristine	6296.81	2.739	79.4	13.686	-
	After hail test	6286.83	2.735	71.2	12.244	-10.53
5BB_BOPET	Pristine	9051.15	1.311	76.7	9.104	-
	After hail test	9062.47	1.306	70.2	8.306	-8.76
10BB_BOPET	Pristine	6198.67	2.729	79.6	13.467	-
	After hail test	6234.66	2.702	63.5	10.689	-20.62
5BB_GLASS	Pristine	9024.09	1.309	78.4	9.265	-
	After hail test	9042.28	1.309	78.3	9.261	-0.04
5BB_GLASS	Pristine	6263.11	2.747	80.6	13.858	-
	After hail test	6268.56	2.747	80.1	13.809	-0.35

2.1.5. Adhesion testing

The adhesion at the encapsulant-skin interface is assessed using the 90° peel tests, as shown in the Fig. 13, below. During the peel test, a pleatuating load between points a and b is taken and divided by the width of the samples to get the peel strength.

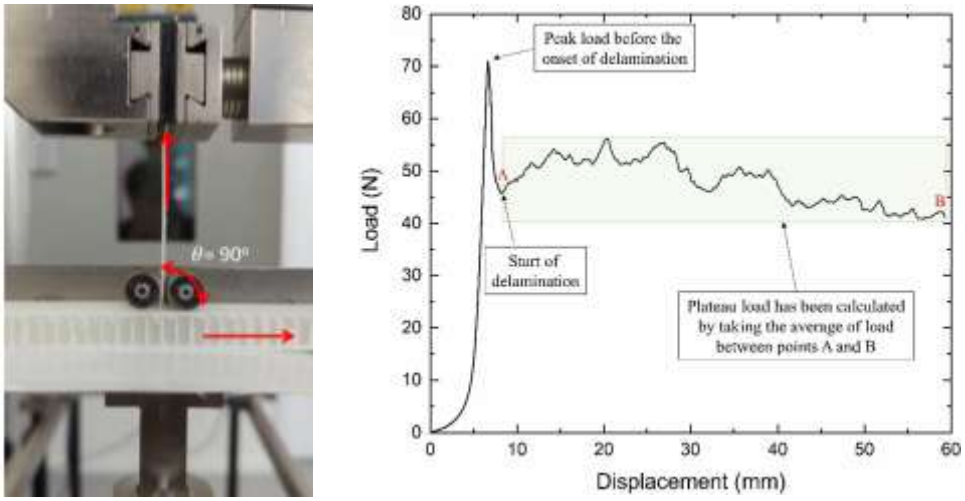

(a) (b)

Fig. 13: (a) set-up for 90° peel tests and (b) characteristic load vs displacement diagram.

For the initial screening of the adhesion strength between the encapsulant and the skins, the samples are tested for both the pristine and the 300 hours DH aged condition. It was observed that the adhesion strength of the PETGF skins was the highest with the encapsulants, while the adhesion to the other skins was unsatisfactory. The adhesion strength was found to reduce slightly after 300 hours of DH ageing; however, the adhesion strength did not reduce for the rest of the samples after the ageing (Fig. 14).

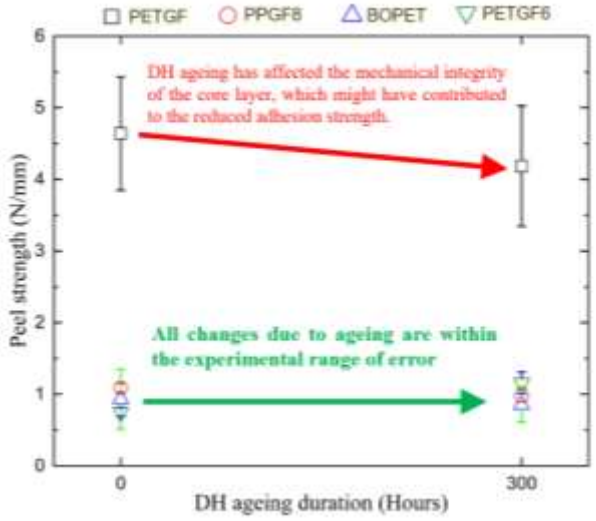

Fig. 14: Effect of 300 hours of DH ageing on the adhesion strength of encapsulant with various skins

Several other factors for the skins such as shrinkage test, water vapor transmittance rate (WVTR), UV ageing and DH ageing of the skins was evaluated by other members of the consortium, as shown below (Table 4):

Table 4 Other aspects of reliability of skins being studied by other consortium members

Factor	Partner investigating it
Shrinkage (CET)	PCCL & OFI
WVTR	OFI
UV ageing	EconCore
DH ageing	PCCL

Based on all the factors studied so far by various partners, a ranking was given to all the four candidate materials during the project meeting held at Genk, Belgium. The ranking matrix suggested that PET-BOPET option of the sandwich, which scored the least among all the candidate materials was decided to be discarded (Table 5).

Table 5: The ranking matrix for various skins being considered

Property	**PET-BOPET**	**PET-GF**	**PP CP660**	**PP CP820**
Adhesion (HC to skin)	0	4	5	5
Adhesion (Encapsulant to skin)	1	4	1	1*
Shrinkage / CTE	2	2	3	4
Water Vapour Transmission Rate	5	4	0	2
UV resistance	1	1	4	0
DH resistance	1	2	4	4
Total	**10**	**17**	**17**	**16**

Furthermore, the adhesion strength measurement was tried by varying the lamination parameters for the BPO encapsulant and the other candidate materials such as Arkema TPO and 3M POE. It was found out that the adhesion strength for the 3M POE was the highest as compared to the rest of the encapsulants, both before and after the DH ageing of 1000 hours (Table 6).

Table 6 Results of peel tests carried out for different lamination parameters and encapsulants at the encapsulant-skin interface

Skin	Encapsulant	Pressure [mbar]	Temperature [°C]	Pristine	DH1000
PPGF8	BPO	300	135	0.22 ± 0.05	0.09 ± 0.07
	BPO	700	135	0.46 ± 0.04	0.38 ± 0.02
	BPO	700	150	0.64 ± 0.04	0.40 ± 0.07
	POE	700	150	3.37 ± 0.46	4.95 ± 0.55
	TPO	700	150	0.64 ± 0.07	0.30 ± 0.03
	EPE	700	150	3.2 ± 0.3	-
PPGF6	BPO	300	135	0.44 ± 0.07	0.36 ± 0.02
	BPO	700	135	0.39 ± 0.00	0.31 ± 0.10
	BPO	700	150	2.05 ± 0.02	0.51 ± 0.05
	POE	700	150	3.33 ± 0.14	3.67 ± 0.50
	TPO	700	150	0.79 ± 0.05	0.62 ± 0.09
	EPE	700	150	3.1 ± 0.2	-

2.2. Change in the bill-of-materials for further testing in the form of mini-modules

Based on the reliability testing performed in the previous round of experiments on the initial candidate materials, it was decided to only focus on developing and testing the modules based on polypropylene based skin/honeycomb sandwich structures. Another key decision taken was regarding selection of encapsulant, where the consortium has decided to use polyolefin elastomer (POE) instead of thermoplastic polyolefin (TPO) due to very low adhesion of TPO with the novel skins.

For performance and aesthetics, the existing bill of materials were reviewed and improved; wherein, PET-based transparent polymeric foil is chosen as front-sheet, polyolefin elastomer is chosen as encapsulant, a coloured polymeric foil is incorporated to improve the aesthetics, M2-size passivated emitter rear contacted cells having five busbars were selected, along with the polypropylene based skin/honeycomb/skin candidates. For the skins, two candidates of different fibre density were selected: 660 g/m^2 (black in appearance, hereafter referred to as PPGF6) and 820 g/m^2 (white in appearance, hereafter referred to as PPGF8). The architecture of such modules is presented in Fig. 15, below.

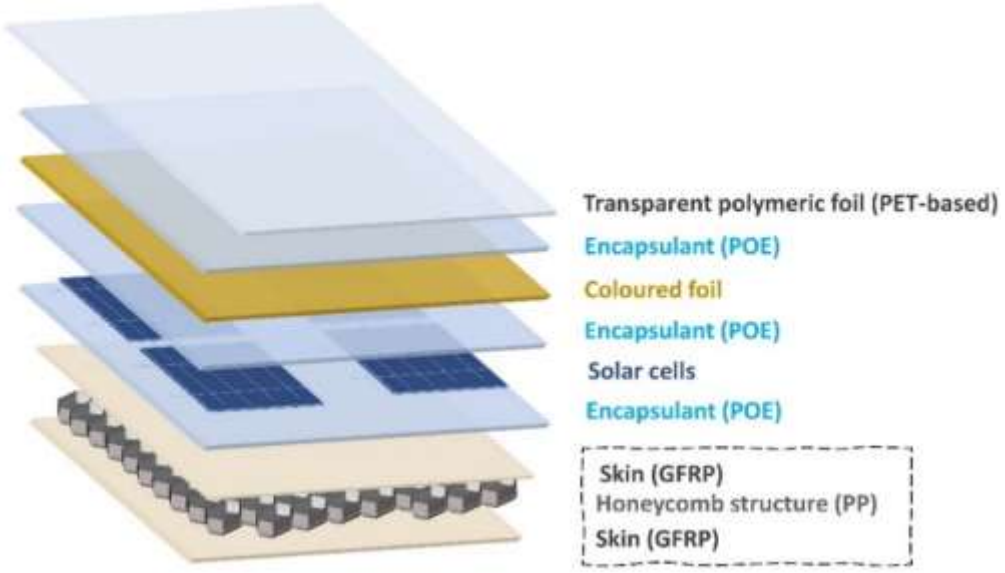

Fig. 15 Structure of the lightweight PV module based on polymeric honeycomb

The prototypes developed as per the bill of materials described above are presented below, in Fig. 16. As can be seen in Fig. 16, the difference in the two skin types changes the overall perception of the coloured foils in the minimodules. The darker background of the PPGF6 skin effectively hides the profiles of the cells, which improves the aesthetics of these mini modules. However, it is evident that the strip used to interconnect the strips is still clearly noticeable, but this can be addressed by the use of a black coloured ribbon. Therefore, it was decided to focus on assessing the reliability of these mini-modules against accelerated climatic ageing, like, damp-heat ageing, thermal cycling, humidity freeze cycling and exposure to ultraviolet ageing. In addition to this, a sample of PPGF8 without any colour was also investigated for its stability against the environmental stressors.

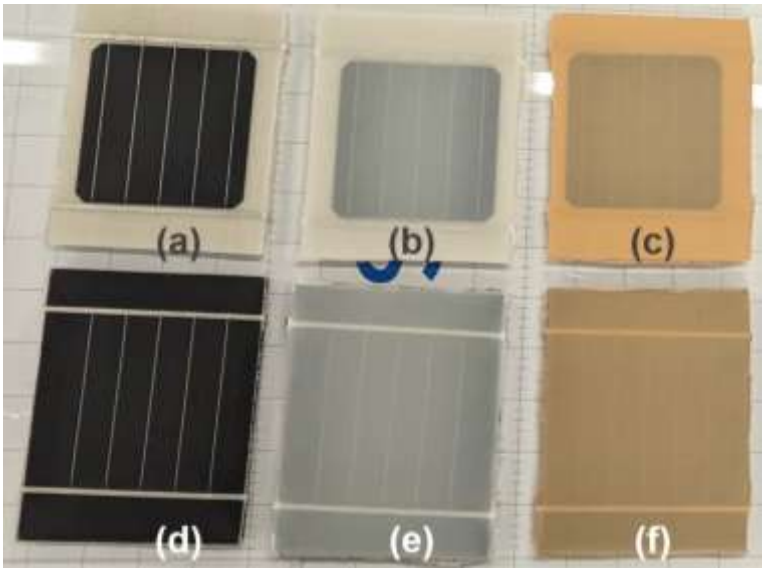

Fig. 16 Mini-modules based on PPGF8 skins with (a) no coloured, (b) dark grey coloured, and (c) beige coloured foils; as well as based on PPGF6 skins with (d) no coloured, (e) dark grey coloured, and (f) beige coloured foils

2.2.1. Reliability testing of mini-modules against climatic stressors

To examine how climatic stressors, such as moisture ingress, UV irradiation, and temperature changes in the real-world scenario, impact the performance of lightweight PV modules, one-cell mini-modules were fabricated and exposed to accelerated artificial tests, as per IEC 61215:2021 standard. These included damp-heat aging at 85°C/85%RH for upto 2000 hours, UV aging at 340nm wavelength with irradiation of 0.8 W/m^2 @ 60°C up to 60 kWh/m^2, 40 humidity-freeze cycles between -40°C and 85°C, and 400 thermal cycles as per IEC 61215 standard, i.e., applied between 85 deg C and -40 deg C, with dwell times and rates of heating and cooling as per the IEC standard. Humidity is maintained at 85 % RH during the time 85 deg C is maintained, otherwise not controlled. In Fig. 17a, the relative maximum power output is plotted against hours of damp-heat aging for these mini-modules. Findings indicate that all modules, except the white-transparent one, showed degradation levels below 5%. In the white-transparent module, a rapid drop in power output occurred due to a busbar breakage, which hindered the use of four-probe contact measurements for IV characterization. This breakage increased the series resistance, resulting in lower power output, which can be regarded as negligible in this context. For the other modules, a slight decrease in power output is mainly attributed to the decline in short-circuit current due to damp-heat aging. Fig. 17b and c present the IV characteristics for the white-transparent and black-transparent samples, respectively. Fig. 17c further shows that the increase in series resistance observed in the white-transparent sample is absent in the black-transparent sample, suggesting it is not associated with cell degradation.

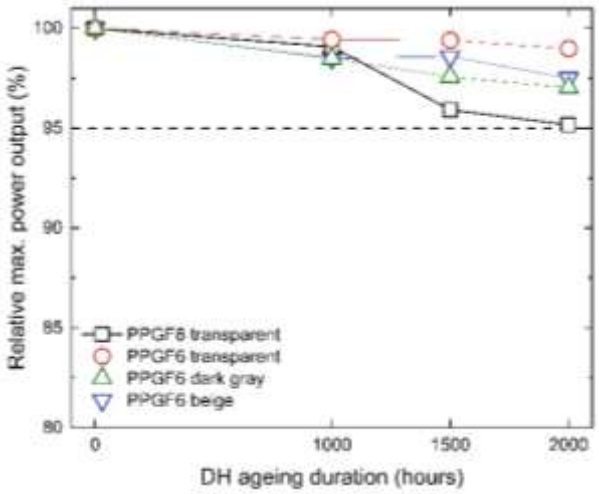

(a)

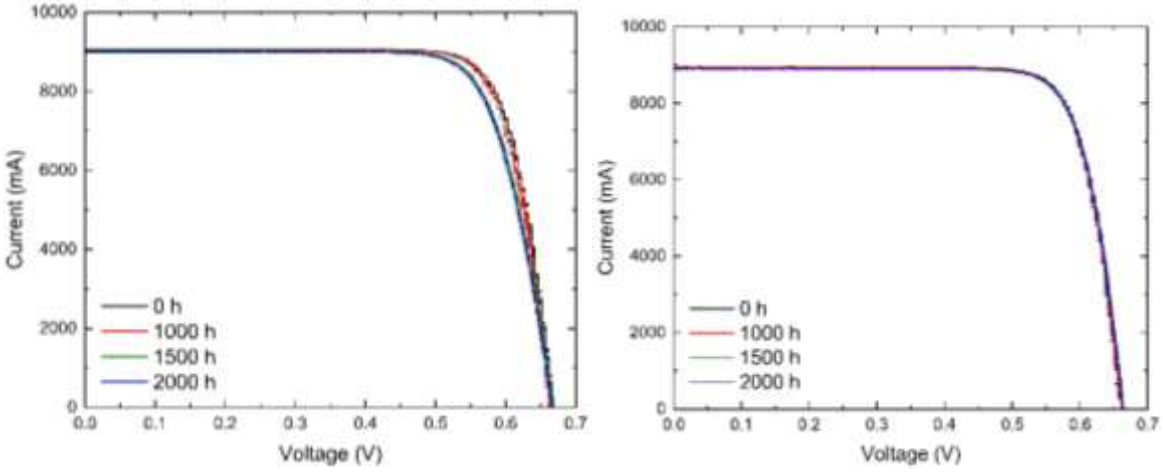

(b)

(c)

Fig. 17 (a): Change in relative max. power output with DH ageing, (b): Evolution of IV characteristics with DH ageing for White-transparent sample and (c) Evolution of IV characteristics with DH ageing for black-transparent sample

The effect of other climatic stressors, like, UV, TC, and HF on the performance of the PV modules is presented in Fig. 18, below. A gradual yet steady decline in power output was observed in the modules exposed to UV irradiation, thermal cycling, and humidity-freeze cycling. It is observed that within the test durations as described in IEC-61215:2021, i.e., 1000 hours of DH ageing, 200 thermal cycling and 20 HF cycles, the reduction in relative max. power output is not significant for these modules after the ageing. It is also required to assess the mechanical response of these modules against the applied loads.

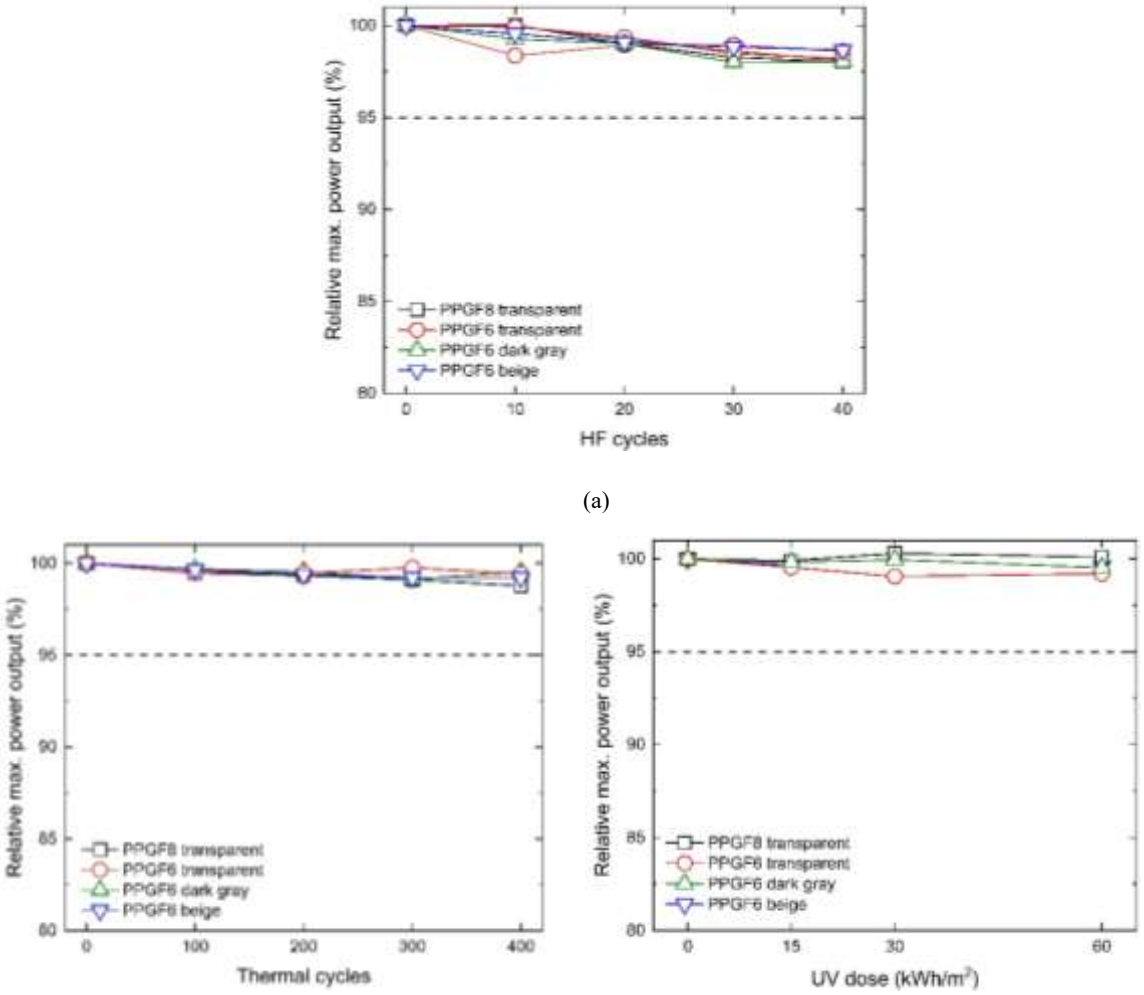

Fig. 18 Evolution of % relative maximum power output with respect to (a) Humidity freeze cycles, (b) thermal cycles and (c) UV dose

2.2.2. Flexural tests

To determine the mechanical stiffness and load-bearing capacity of two composite backsheets, flexural testing was performed using a four-point bending setup. Samples with a width of 25 mm were tested under a loading rate of 20 µm/s, using an outer span of 190 mm and an inner span of 90 mm (Fig. 19a). The flexural properties were analyzed in two orientations for each backsheet: the longitudinal (L) direction, which aligns with the bonded walls of the honeycomb structure, and the transverse (T) direction, which is perpendicular to this alignment (illustrated in Fig. 19b).

Fig. 19 (a) The set-up used for four-point bending and (b) indication of two mutually perpendicular directions, longitudinal (L) and transverse (T) of the honeycomb along which the testing is done

The results of the four-point bending tests for sandwich structures with a skin/HC/skin configuration, as shown in Fig. 20. The results indicate that the PPGF8 structure exhibits greater bending stiffness than the PPGF6 structure, attributed to the higher fibre density in the PPGF8 skins. Flexural properties were evaluated for both types of samples in the longitudinal and transverse directions of the honeycomb core. The tests revealed that both sandwich structures possess higher flexural stiffness along the longitudinal direction than the transverse direction. This finding highlights the anisotropic properties of the honeycomb core, leading to approximately a 50% reduction in the structure's maximum load-bearing capacity when bending occurs in the transverse direction compared to the longitudinal direction.

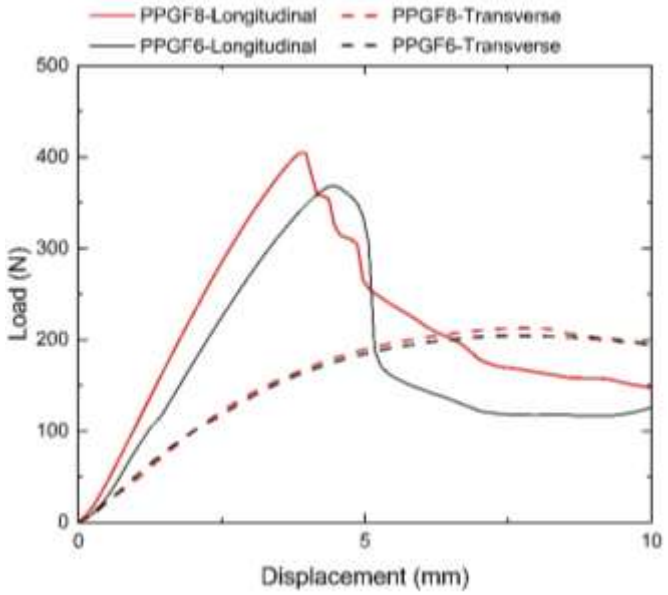

Fig. 20 Comparison of flexural bending behaviour for PPGF6 and PPGF8 samples along both longitudinal as well as transverse direction

2.2.3. Static mechanical load tests on mini-modules

To assess the mechanical response of modules with PPGF8 and PPGF6 backsheets, static mechanical load tests were conducted on mini-modules with dimensions of 40 cm x 40 cm, each consisting of four series-connected cells. These modules were securely clamped onto a metallic frame, as shown in Fig. 21a and Fig. 21b, and pressure was applied using vacuum cups. Two distinct loading cycles were used to analyse the modules' behaviour.

In type 1 loading, three cycles with an amplitude of 2400 Pa and a mean pressure of 0 Pa were applied, while type 2 loading involved a sequence of one cycle at 5400 Pa and another at 8000 Pa, both with a mean pressure of 0 Pa. Each loading cycle was held at maximum load for a duration of 1 hour. Type 1 loading was performed on both PPGF8 and PPGF6 samples, whereas type 2 loading was specific to PPGF8. To verify electrical continuity, a 1A current was applied and monitored throughout the tests. Displacement at the centre of the modules was measured using a spring-loaded sensor positioned at the back, as depicted in Fig. 21c. The corresponding electroluminescence (EL) images and load-displacement curves for these modules are presented in Fig. 22 and, Fig. 23, below. It appears that the loading cycles did not result in any major crack formation after the loading.

(a)

(b)

(c)

Fig. 21 LW modules based on (a) PPGF8 and (b) PPGF6, under static mechanical loading, (c) attachment of a spring-loaded displacement sensor at the back of a module's centre. To keep track of any possible circuit disconnection, the modules were subjected to 1 A current.

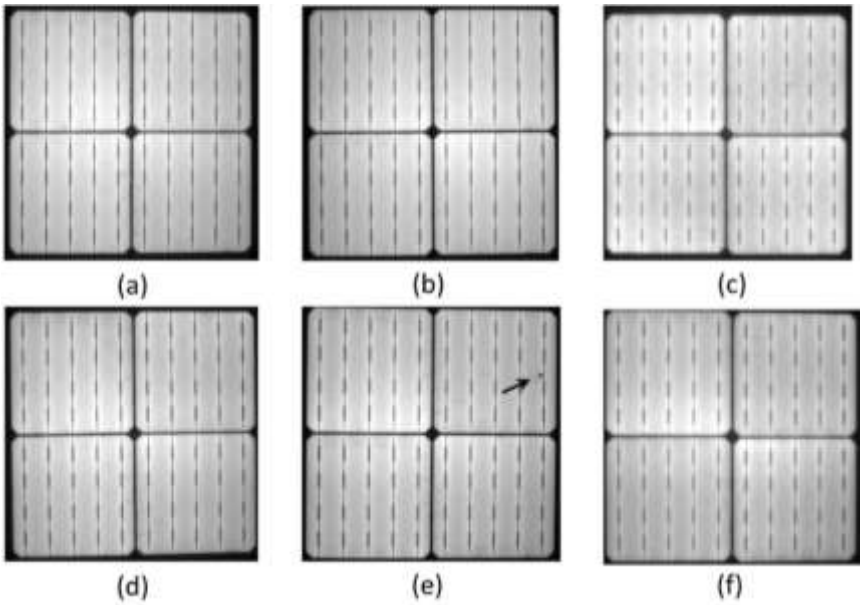

Fig. 22 EL images of mini-modules for (a) PPGF8 and (b) PPGF6 in the pristine condition & after applying type 1 loading cycles on (d) PPGF8 and (e) PPGF6. Furthermore, EL images of mini-modules consisting PPGF8 (a) before and (f) after applying type 2 loading cycles

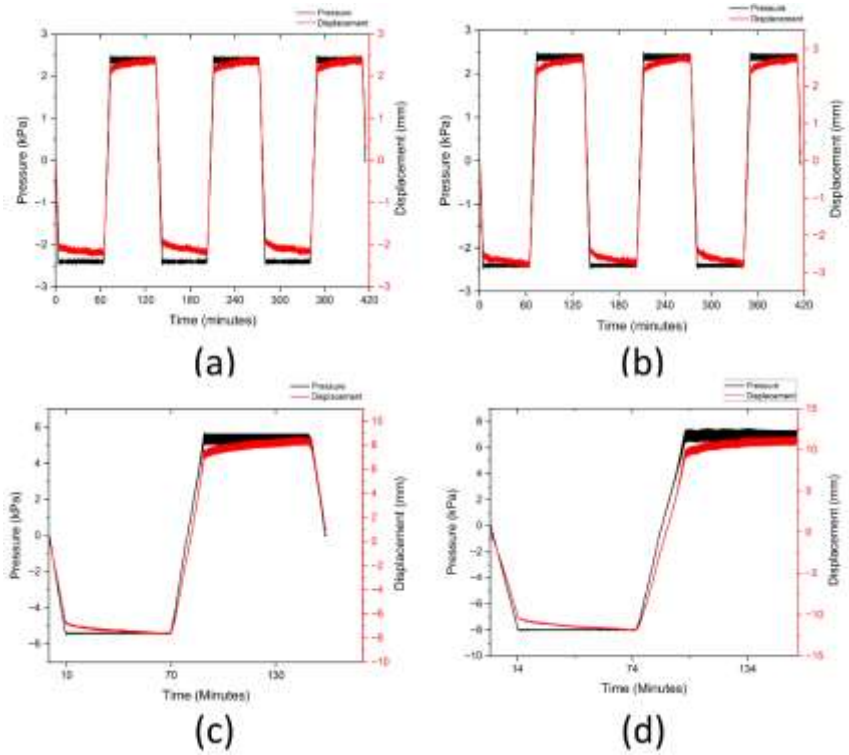

Fig. 23 Evolution of pressure and displacement profiles with time for the mini modules subjected to type 1 loading based on (a) PPGF8 type backsheet and (b) PPGF6 type backsheet; and type 2 loading on PPGF8 based backsheet for amplitude of (c) 5400 Pa and (d) 8000

2.2.4. Flammability tests on mini-modules

To assess fire performance, two types of sandwich structures were subjected to flame exposure to observe behaviours such as flaming droplet production, smoke generation, and flame spread from the point of contact (Fs). The objective was to determine if the samples meet the requirements of Class 'E' according to ISO 11925, which stipulates that Fs must remain below 150 mm. During testing, a flame composed of 30% propane and 70% butane was applied to each specimen for 15 seconds, then removed, followed by a 5-second wait before extinguishing.

The instances of maximum flame spread (Fs) within the 20-second test duration are presented in Fig. 24. For the PPGF8-based sandwich structure, Fs remained below 150 mm, while for the PPGF6-based structure, it reached approximately 170 mm. Both samples exhibited flaming droplets within the 20-second test period, suggesting a need for enhanced fire resistance in these composite backsheets, potentially through the addition of fire retardants or other modifications.

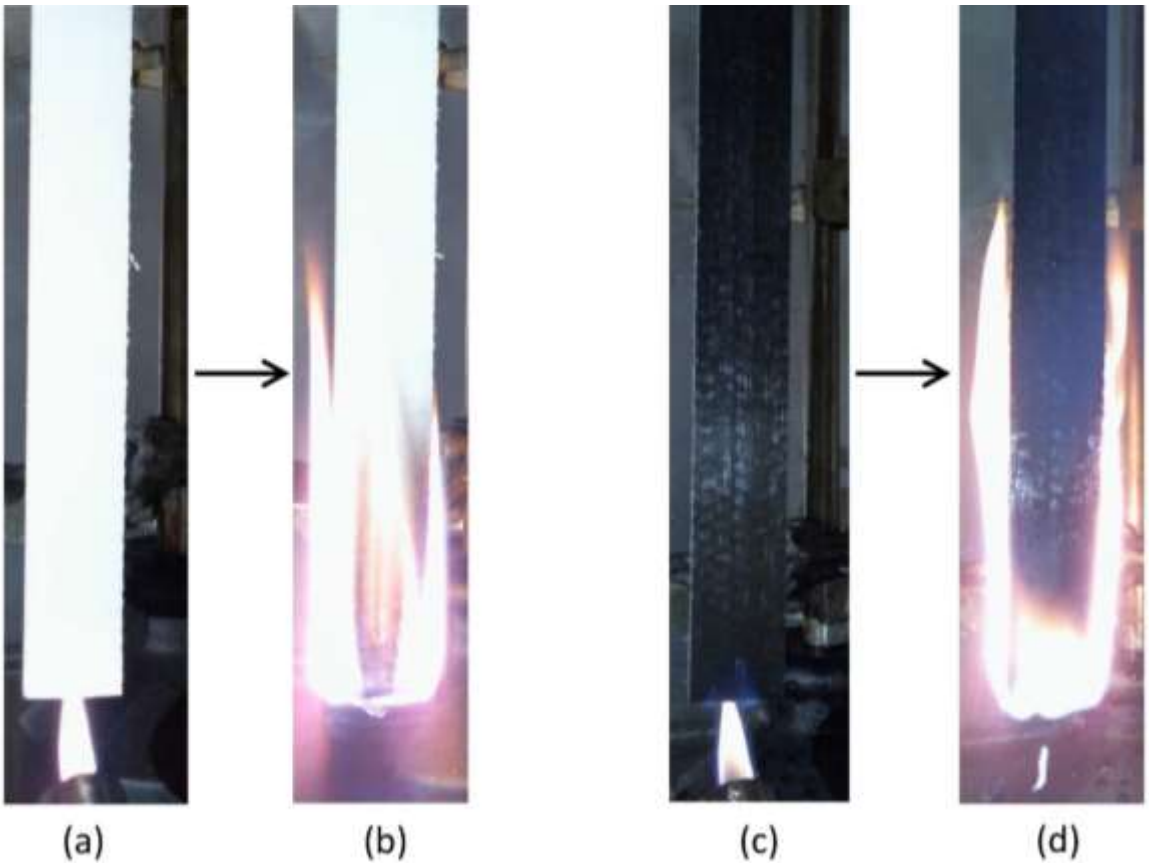

Fig. 24 Flammability tests for PPGF8 based backsheets (a) before the test and (b) at the instance when the flame propagation is the highest; and for PPGF6 based backsheets (a) before the test and (b) at the instance when the flame propagation is the highest

Mini-PV modules based on both the polypropylene based skins were also subjected to flammability tests and the results are shown in Fig. 25. It appears that the damage due to the flame is almost the same and the edge and the front of the modules sustained the greatest damage.

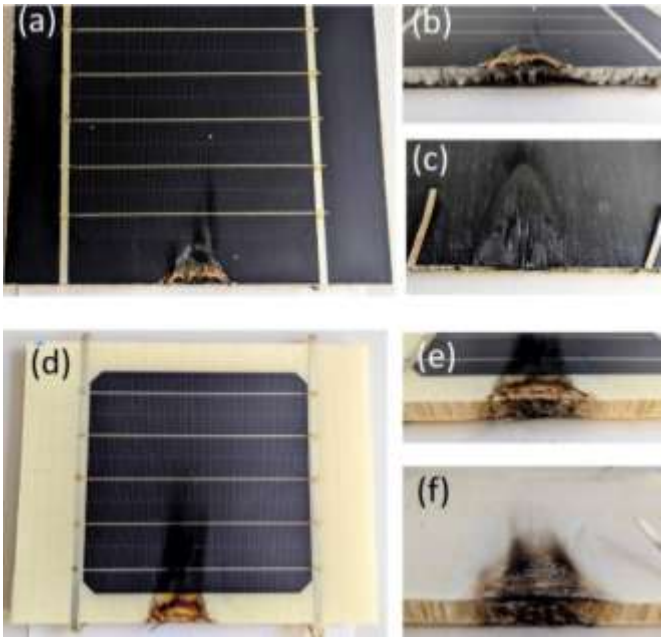

Fig. 25 Visual appearance of the mini-PV modules based on PPGF6 are shown in (a, b and c); while the same is indicated in for PPGF8 in (d, e, and f).

2.3. Reliability testing on modules of larger format: effect of sequential ageing

As discussed in the section 2.2.1, the chosen bill of materials performed well against the individual stressors like, damp heat, UV aging, thermal cycling and humidity freeze. It was observed that the degradation in power output of the minimodules remained less than 5% through the testing. However, in the outdoor conditions, all the stressors like, UV, TC, humidity ingress and mechanical loads act together; therefore, in this section accelerated sequential ageing of various type have been applied on the modules of larger format. The three sequences studied are as mentioned below:

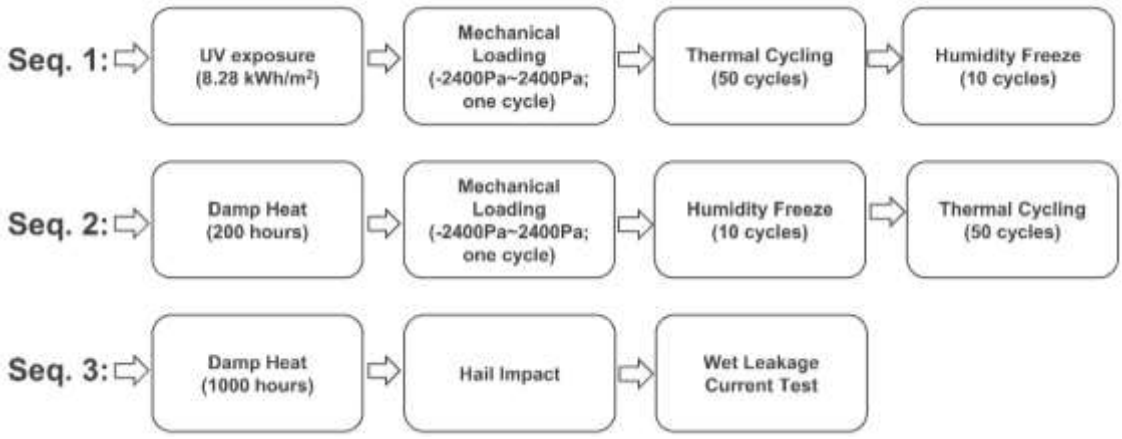

Fig. 26: The three sequences used for studying the effect of combination of various climatic stressors

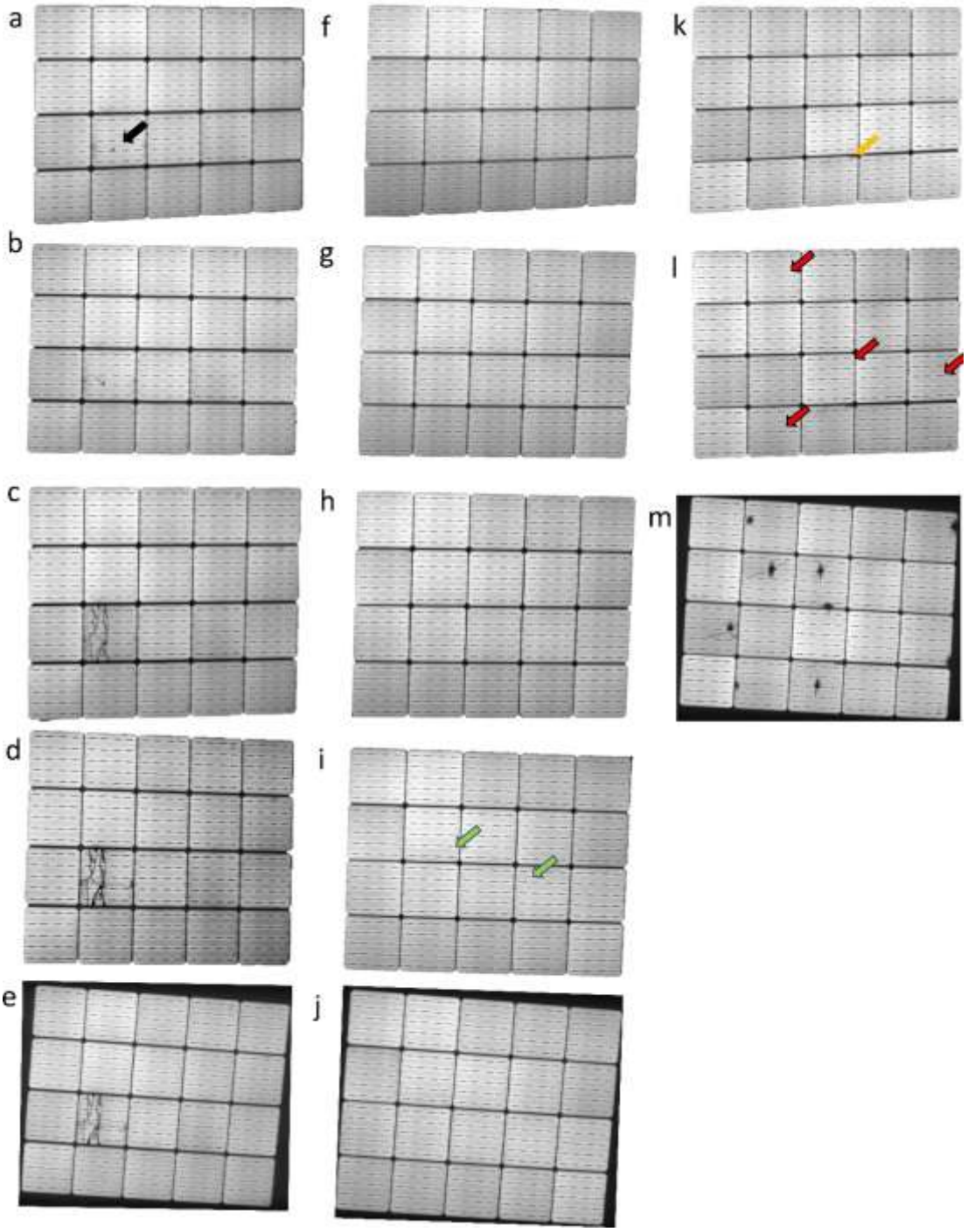

Fig. 27: EL images of the module subjected to sequence 1 in (a) pristine condition, (b) after UV exposure, (c) after mechanical loading, (d) after thermal cycling, (e) after humidity freeze cycling; for module subjected to sequence 2 in (f) pristine condition, (g) after DH, (h) after mechanical loading, (i) after humidity freeze cycling, (j) after thermal cycling; and for module subjected to sequence 3 in (k) pristine condition, (l) after DH ageing and (m) after hail impact test

The EL images and IV curves for the modules based on these three sequences are presented in Fig. 27 and Fig. 28, respectively. The IV characteristics of the modules are also tabulated in Table 7. It is found that in the module used for exposure to sequence 1, a microcrack was present in the pristine condition which got elongated as the ageing proceeded. However, no major degradation signatures were found on this module. On the other hand, for the module subjected to sequence 2, only after the humidity freeze cycling finger failure of a few cells was observed (as highlighted with green-colored arrows in Fig. 27 i). Sequence 3 which comprises of DH ageing followed by hail impact test showed large inactive cell areas (seen as the black colored area in EL image Fig. 27 m). Overall, as can be seen in Table 7, the power output degradation remains less than 5% in all the three-sequence tested. Notably for the module tested under sequence 3, after the hail impact tests, the power output reduces by as much as 3.99 %. The wet-leakage current tests carried out in the study indicated that the modules pass the criteria (i.e., insulation resistance of more than 40 MJ/m^2). Therefore, it can be concluded that these modules have successfully passed the three sequences as the power output degradation remains less than 5% in all the cases.

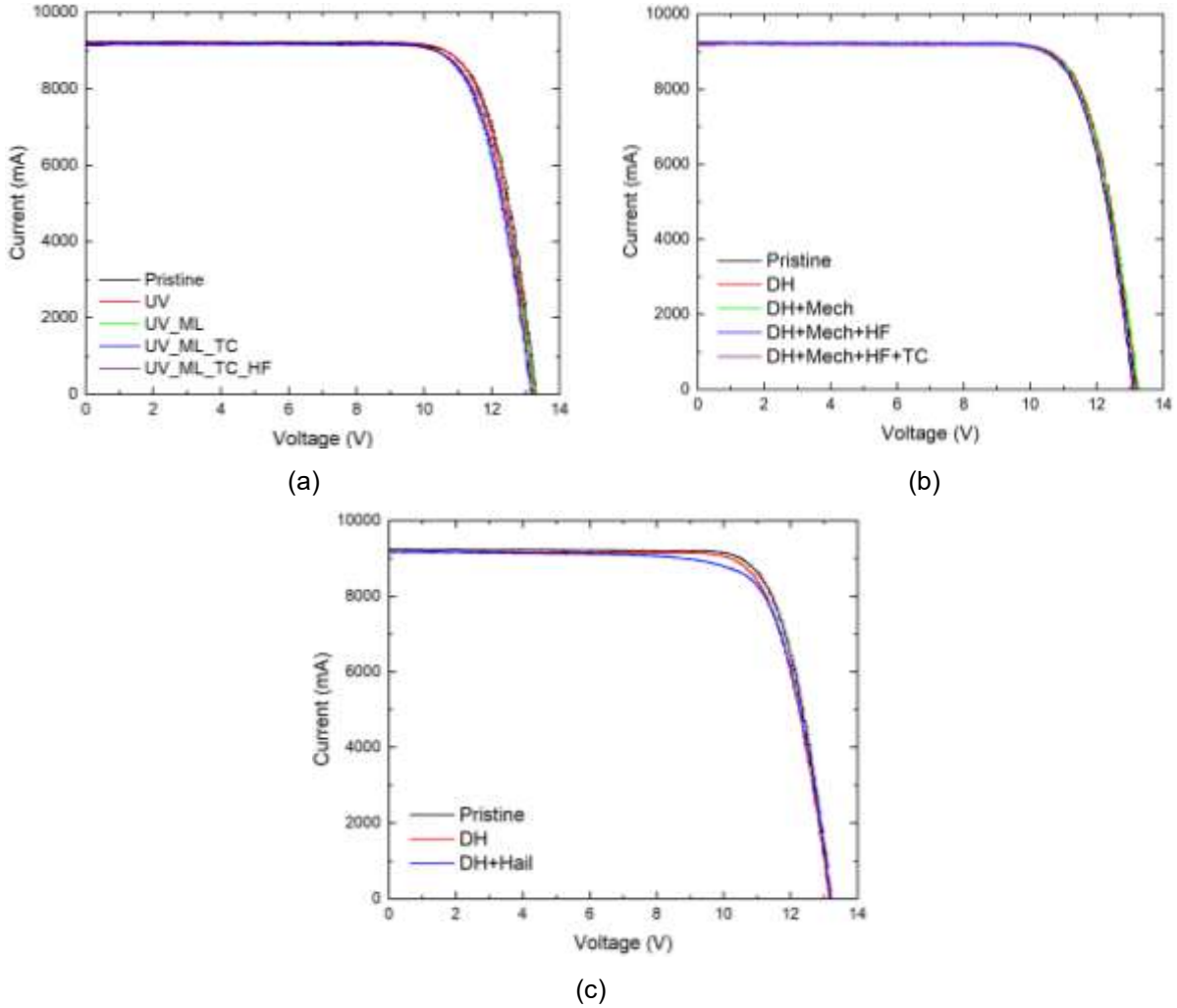

Fig. 28: IV curves for modules subjected to sequence 1 (a), sequence 2 (b) and sequence 3 (c).

Table 7: IV characteristics of the modules subjected to sequence 1, 2 and 3

Sequence	Conditions	Isc (A)	Voc (V)	FF(%)	Pmax (W)	Rs (Ω)
Sequence 1	Pristine	9.18	13.32	79.1	96.73	0.147
	UV	9.24	13.25	78.9	96.59	0.146
	UV+ML	9.22	13.26	77.5	94.72	0.164
	UV+ML+TC	9.21	13.18	77.9	94.51	0.161
	UV+ML+TC+HF	9.16	13.13	78.52	94.44	0.15
	(% Change)	**-0.21**	**-1.4**	**-0.72**	**-2.4**	**2.04**
Sequence 2	Pristine	9.23	13.18	78.9	95.92	0.144
	DH	9.23	13.23	78.9	96.3	0.15
	DH+ML	9.23	13.26	78.4	95.87	0.155
	DH+ML+HF	9.25	13.11	78.9	95.62	0.149
	DH+ML+HF+TC	9.19	13.08	79.01	94.98	0.15
	(% Change)	**-0.43**	**-0.75**	**0.14**	**-0.98**	**4.16**
Sequence 3	Pristine	9.23	13.22	78.2	95.48	0.154
	DH	9.18	13.18	77.6	93.81	0.167
	DH+Hail	9.17	13.19	75.79	91.67	0.17
	(% Change)	**-0.65**	**-0.23**	**-3.08**	**-3.99**	**7.14**

2.4. Development of novel coatings for frontsheet and its reliability testing

Delight consortium partner Rembrandtin with the support of OFI developed novel coating solutions for frontsheets that can be UV cured to impart protection to the PET core layer of the commercially available frontsheets from manufacturers like, COVEME or MYLAR, for example.

2.4.1. Reliability testing on the free-standing frontsheets with coatings

For the development of new frontsheet coatings the focus was set on UV curable coating systems. Four different UV-curing coating systems were developed and applied to PET carrier films. Different acrylate monomers (type A and B) and urethane-acrylate oligomers in combination with (i) UV-absorbers and (ii) moisture barrier pigments were used for these UV-curable coatings. The monomers used are almost comparable in their viscosity. However, they differ in their glass transition temperature (Tg), which is higher for monomer A (used for sample F1) than for monomer B (used for samples F2, F3 and F4). The chosen coating material is a 100% system, which means that no solvents are required and therefore no volatile organic compounds (VOCs) are released. Detailed information on the samples is given in

Table 8. Commercial PET frontsheets with ETFE coating were used as reference material/benchmark.

Table 8: Samples overview

Sample ID	Foil	Monomer A	Monomer B	Oligo-mer	UV-Absorber	Barrier pig-ment
F0	PET Mylar 204	-	-	-	-	-

F1	PET Mylar 204	x	-	x	-	-
F2	PET Mylar 204	-	x	x	-	-
F3	PET Mylar 204	-	x	x	x	-
F4	PET Mylar 204	-	x	x	x	x
R	Used as reference: PET with ETFE coating (commercial frontsheet)					

For achieving a better adhesion of the coating materials to the PET surface, the PET carrier films were subjected to a corona treatment (carried out on both sides of the PET film) with each side being treated for 5 seconds at a nominal power of 300 W. In the next step, the coating was manually applied to the PET film using a spiral film applicator to achieve the desired coating thickness of 30 µm – 50 µm. After application of the coating on the corona-pre-treated PET substrate, it was cured using UV-light (mercury vapor lamp 180-450 nm, dose 1200 mJ/cm², curing time 30 seconds). Material characterization was done at first visually: it was found that the coating was applied homogeneously and without defects such as bubbles, cavities or delamination. The cross-cutting test after coating application revealed very good adhesion between coating and PET substrate (Fig. 29).

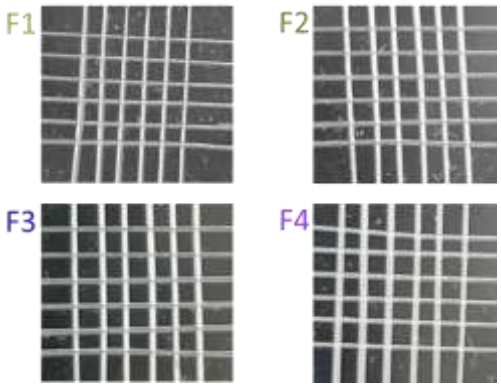

Fig. 29: Light microscopic images; cross-cut for samples after coating application

Since providing high transparency is one of the main requirements for a PV frontsheet material, in the next step optical analysis using UV-VIS-NIR spectroscopy have been performed and the effective transmission T' was calculated for each material. As can be seen from Fig. 30, the coating has an impact on the transmission: samples F1, F3 and F4 exhibit slight transmission losses, whereas sample F2 only shows minimal losses, mostly at lower wavelengths of the VIS range.

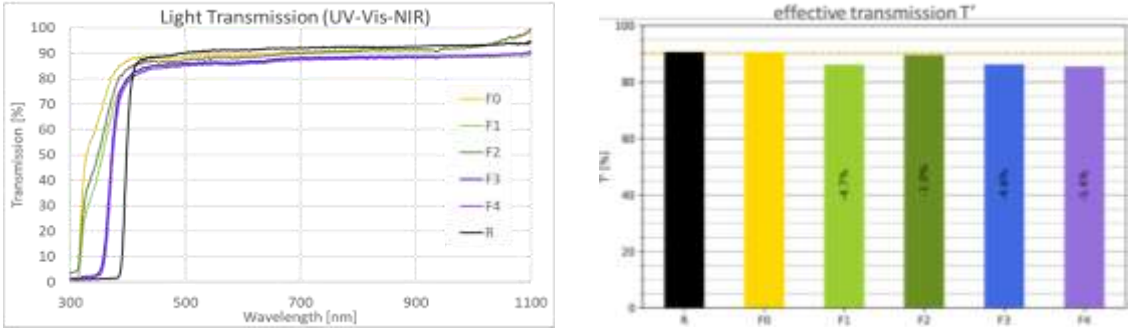

Fig. 30: Transmission curves of the pure PET foil (F0), the coated samples F1 - F4 and - for comparison - the reference samples R (PET+ ETFE)

As moisture ingress in PV modules is a critical factor for performance degradation, WVTR measurements were carried out on development frontsheets. The results are depicted in Fig. 31, showing the

WVTR in [g/(m2.d)] for the various coated PET-foils (without normalization to the sample thickness). As all coated PET foils give identical WVTR values - irrespective of the coating type and thickness - and are also equal to the WVTR of the uncoated sample, it can be concluded that the permeability of the PET foils determines the overall WVTR of the coated frontsheets.

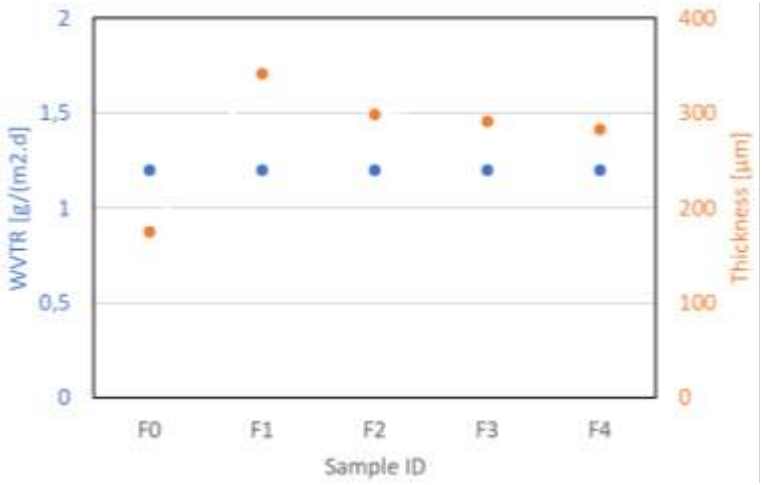

Fig. 31: WVTR of the uncoated PET sample F0 and the coated samples F1-F4

2.4.2. Reliability testing of minimodules containing frontsheets coated with novel coatings

This section deals with reporting the results of the reliability testing done on the minimodules containing the frontsheets coated with different coatings as per the discussion in the section 2.4.1. The EL images for minimodules before and after the UV ageing and DH ageing are presented in Fig. 32 and Fig. 33, respectively while the IV characteristics are presented in Table 9 for UV aged samples and in Table 10 for DH aged samples.

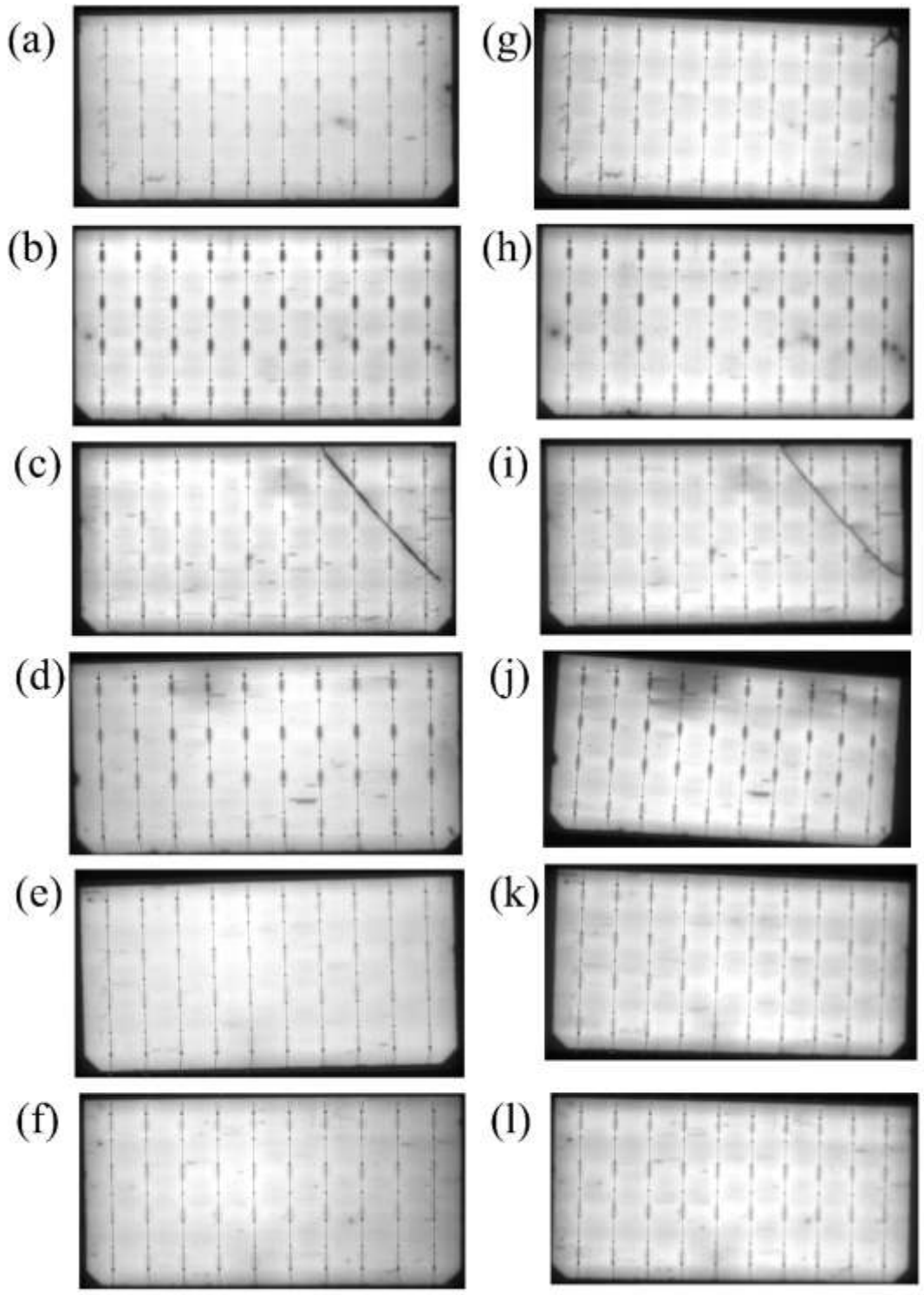

Fig. 32: EL images of minimodules in the pristine condition for sample ID (a) R, (b) F0, (c) F1, (d) F2, (e) F3, (f) F4 and after UV ageing for sample ID (g) R, (h) F0, (i) F1, (j) F2, (k) F3, (l) F4. The sample ID are identified in Table 8.

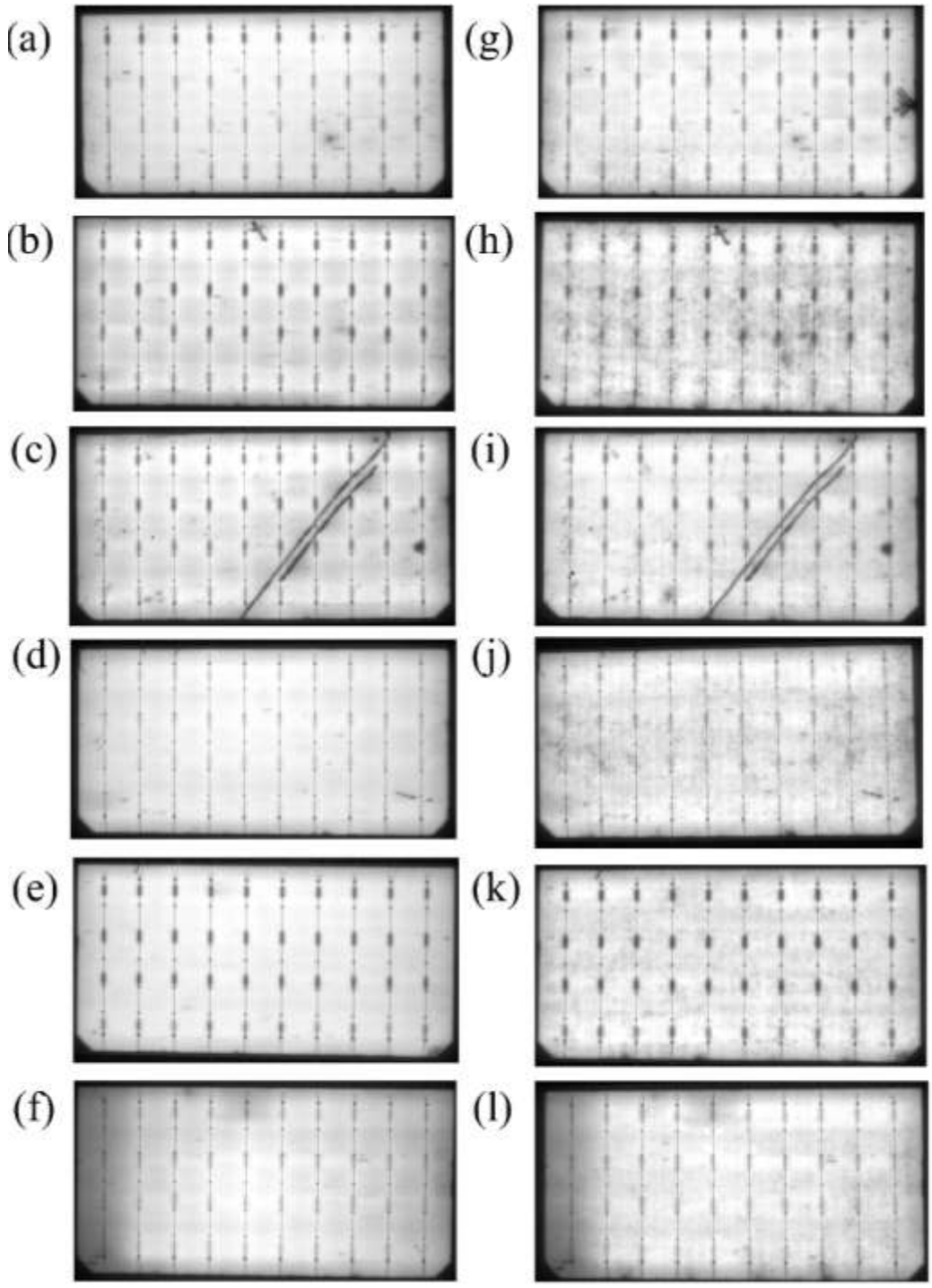

Fig. 33: EL images of minimodules in the pristine condition for sample ID (a) R, (b) F0, (c) F1, (d) F2, (e) F3, (f) F4 and after DH ageing for sample ID (g) R, (h) F0, (i) F1, (j) F2, (k) F3, (l) F4. The sample ID are identified in Table 8.

Table 9: IV characteristics before and after the UV ageing for various samples

Sample ID	Condition	Voc (V)	Isc (mA)	Max Power (mW)	FF (%)
R	Pristine	0.68	6404	3496	80
	After UV ageing	0.69	6432	3512	79.58
	Rel. % change	0.531	0.42	0.46	-0.49
F0	Pristine	0.68	6387	3476	80.2
	After UV ageing	0.68	6353	3451	79.85
	Rel. % change	0.207	-0.53	-0.72	-0.39
F1	Pristine	0.69	6427	3435	77.7
	After UV ageing	0.68	6426	3490	79.38
	Rel. % change	-0.47	-0.01	1.57	2.05
F2	Pristine	0.68	6441	3488	79.1
	After UV ageing	0.68	6418	3470	79.08
	Rel. % change	-0.114	-0.34	-0.51	-0.04
F3	Pristine	0.68	6449	3521	79.8
	After UV ageing	0.69	6461	3538	79.77
	Rel. % change	0.281	0.19	0.47	0.005
F4	Pristine	0.68	6404	3496	79.7
	After UV ageing	0.69	6440	3520	79.62
	Rel. % change	0.281	0.55	0.68	-0.15

Table 10: IV characteristics before and after the DH ageing for various samples

Sample ID	Sample Name	Voc (V)	Isc (mA)	Max Power (mW)	FF (%)
R	Pristine	0.68	6419	3484	79.53
	After DH ageing	0.68	6414	3422	78.69
	Rel. % change	-0.67	-0.07	-1.79	-1.06
F0	Pristine	0.68	6401	3477	79.51
	After DH ageing	0.68	6363	3356	77.54
	Rel. % change	-0.43	-0.58	-3.47	-2.49
F1	Pristine	0.68	6473	3357	75.9
	After DH ageing	0.68	6333	3345	77.82
	Rel. % change	-0.66	-2.17	-0.35	2.53
F2	Pristine	0.68	6449	3538	80.39
	After DH ageing	0.68	6303	3383	78.79
	Rel. % change	-0.2	-2.26	-4.4	-1.99
F3	Pristine	0.68	6434	3475	79.71
	After DH ageing	0.68	6347	3358	78.26
	Rel. % change	-0.22	-1.36	-3.37	-1.82
F4	Pristine	0.68	6449	3475	78.72
	After DH ageing	0.68	6361	3387	77.92
	Rel. % change	-0.18	-1.36	-2.54	-1.02

Overall, from the EL images (Fig. 32) it can be concluded that all the coating solutions perform at par to the commercially available frontsheet 'R' against UV ageing. A slightly higher degradation in power output is observed for the frontsheets coated with F2 type of coating than the others. Looking at the EL images presented in Fig. 33, it can be easily observed that the novel coatings don't protect well the packaged solar cells against the moisture induced degradation, which is present in the form of cell darkening. The IV characteristics for DH aged modules are also tabulated in Table 10, which shows that the coating solution of ID 'F2' has highest degradation in power output close to about 4.4%. Therefore, it can be identified that the monomer B performs poorly as compared to monomer A. Furthermore, stabilization of monomer B containing films with either UV blocker (F3) or UV blocker + barrier pigments (F4) slightly improved the performance but still performed poorly as compared to monomer A containing coatings without any stabilization. Therefore, it can be said that the monomer F1 has greater suitability towards application as a protective coating on the PET based foils as compared to the coatings containing monomer B.

2.5. Design and fabrication of large sized LW modules for demonstration site at microcity, Neuchatel, Switzerland

Accelerated environmental aging tests have shown that the packaging materials used in these lightweight PV modules effectively shield the solar cells from environmental stress, limiting the maximum power output degradation to less than 5%. Based on these promising results, larger modules were fabricated using the previously specified materials and are ready to be exposed to the Central European climate in Neuchâtel, Switzerland. The design of these modules, as shown in Fig. 34, includes 40 series-connected solar cells and four bypass diodes (BPDs), with each BPD connected in parallel to a set of 10 cells. The modules were built with either beige or dark grey colored foils, or with no color foil, as illustrated in Fig. 35. Additionally, colored modules based on dark gray and beige foils are also fabricated for the comparison of aesthetics.

Electroluminescence (EL) images, as well as IV characteristics, are displayed in Fig. 36 and Fig. 37, respectively. Key electrical parameters, such as short-circuit current, open-circuit voltage, maximum power output, and efficiencies, are summarized in Table 11 for these modules.

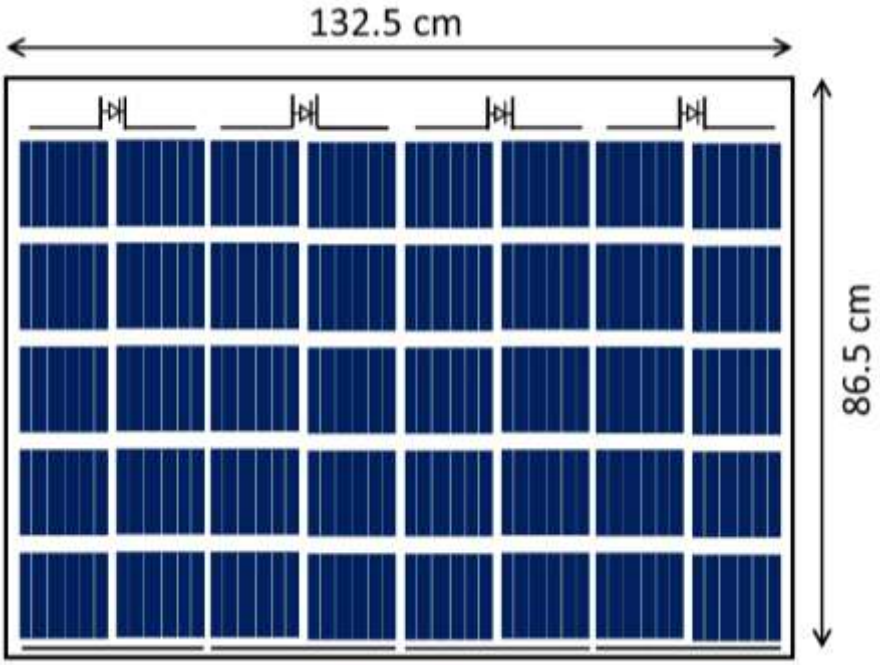

Fig. 34 Design of an upscaled module consisting of 40 series connected cells

Fig. 35 Upscaled modules based on both PPGF8 and PPGF6 skins. The modules with beige and dark grey coloured foils are based on PPGF6 skins.

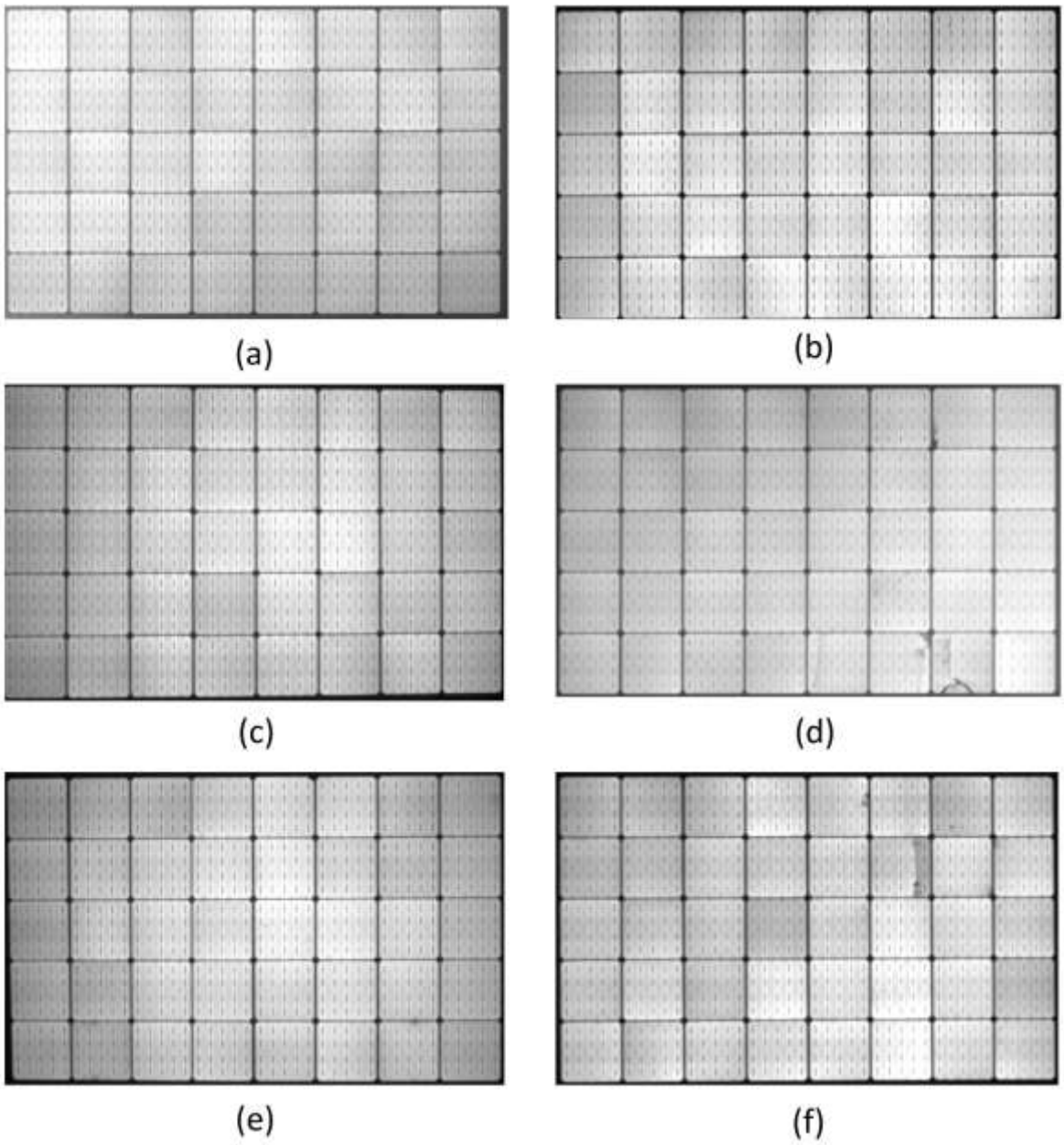

Fig. 36 EL images for modules based on (a) PPGF8 without coloured foil, (b) PPGF6 without coloured foil, (c) PPGF6 with dark grey coloured foil, and (d) PPGF6 with beige coloured foil.

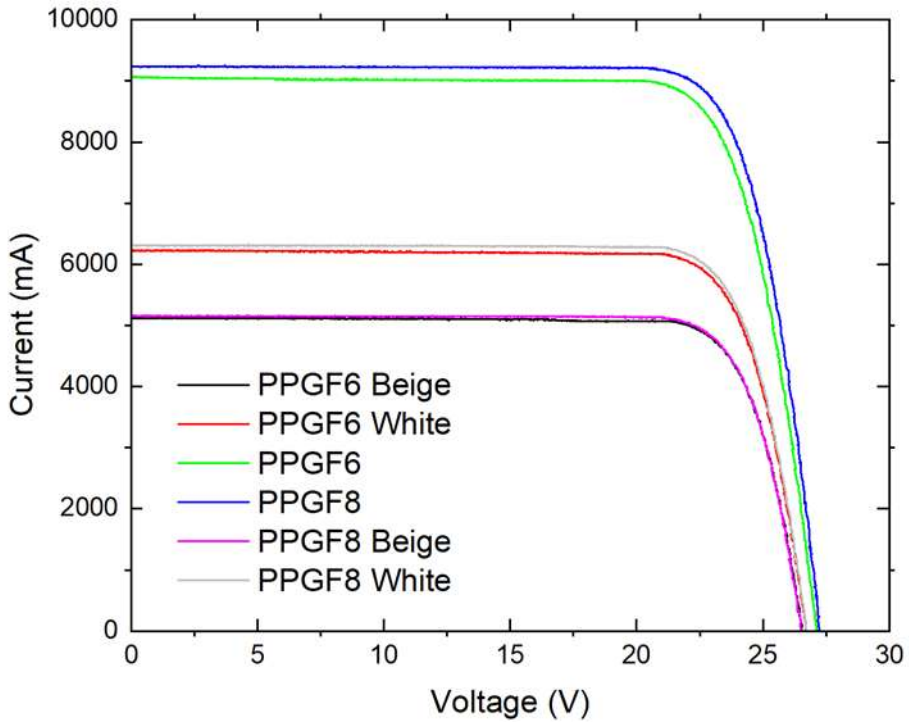

Fig. 37 IV characteristics for upscaled modules

Table 11 Electrical parameters for upscaled modules

Module	Isc (mA)	Voc (V)	Max. Power (W)	Efficiency (%)
PPGF8-Transparent	9122	27.1	195.74	19.57
PPGF6-Transparent	9065	27.1	193.61	19.36
PPGF6-Dark Gray	6215	26.7	134.08	13.4
PPGF6-Beige	5112	26.5	110.94	11.09
PPGF8-Dark Gray	6305	26.7	136.18	13.6
PPGF8-Beige	5220	26.5	112.8	11.19

2.2.7 Set-up of demo site at microcity

A demonstrator test site is being realized on the rooftop of microcity building at Neuchâtel, Switzerland as shown in Fig. 38. This demonstrator will have above-described modules mounted in the form of a façade. The modules will be oriented towards the East direction. Several important outdoor weather data such as, global horizontal irradiance, direct normal irradiance, wind speed, air temperature, etc will be recorded as well. It is planned to monitor the modules in maximum power point (MPP) tracking mode of operation and take time to time indoor characterization to understand if the modules are undergoing degradation during their outdoor operation or not.

Fig. 38 Demonstrator site on microcity rooftop at Neuchatel, Switzerland

The demo site also showcases, for a comparison purpose, two modules based on white skins with colored foils. The goal behind this is to compare aesthetical aspects on the modules of larger format in outdoor condition when installed in the form of a façade. Besides this, another goal of installing these two modules was to compare the energy generated with the modules of the same color that uses black skins.

The power output profiles and plane of array (POA) irradiance profiles are shown in Fig. 39 for a clear day. The irradiance and the corresponding power output of the modules peaks in around 9h30 in the morning since the modules are facing East direction. Furthermore, the power output profiles of the PPGF6-Beige module does not appear to be smooth since it gets shaded due to the nearby railing which activates the bypass diodes. Fig. 40 shows power output profiles for the modules over several days in the summer months.

The modules were taken indoors for characterization after three and nine months of outdoor exposure. The corresponding EL images and IV characteristics are presented in Fig. 41 and Table 12, respectively. It appears that a couple of modules (i.e., PPGF6-Beige and PPGF6-white) had partially cracked cells in the pristine condition which got intensified during the outdoor exposure or handling. Furthermore, for the PPGF8, PPGF8-white and PPGF8-beige modules new cracks appear after the installation and can be noticed that the cells close to the corner seemingly have higher chances of failure. This could partly be due to the mounting induced pressure acting close to the corners of the modules. However, PPGF6 module appears to be completely crack free even after 9 months of outdoor exposure and showed about 1.29 % power output degradation, which is expected as generally modules show maximum degradation during the initial year of the installation.

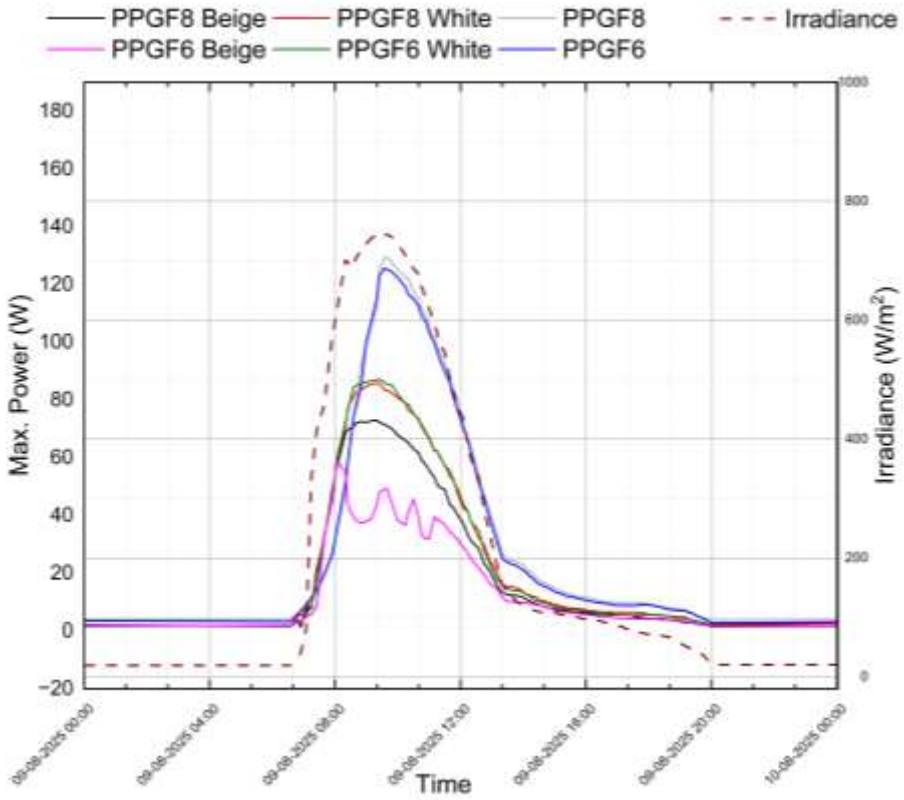

Fig. 39: Irradiance and max power output profiles for the modules mounted in the form of East facing facade

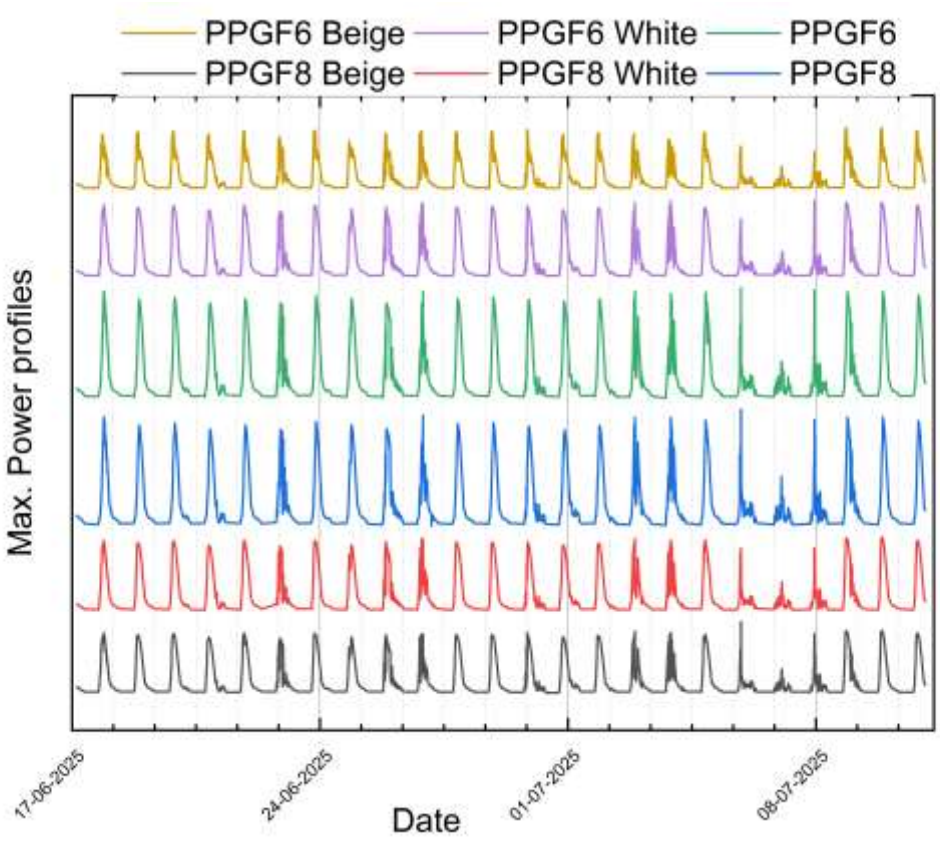

Fig. 40: Power output profile over several days during summer months

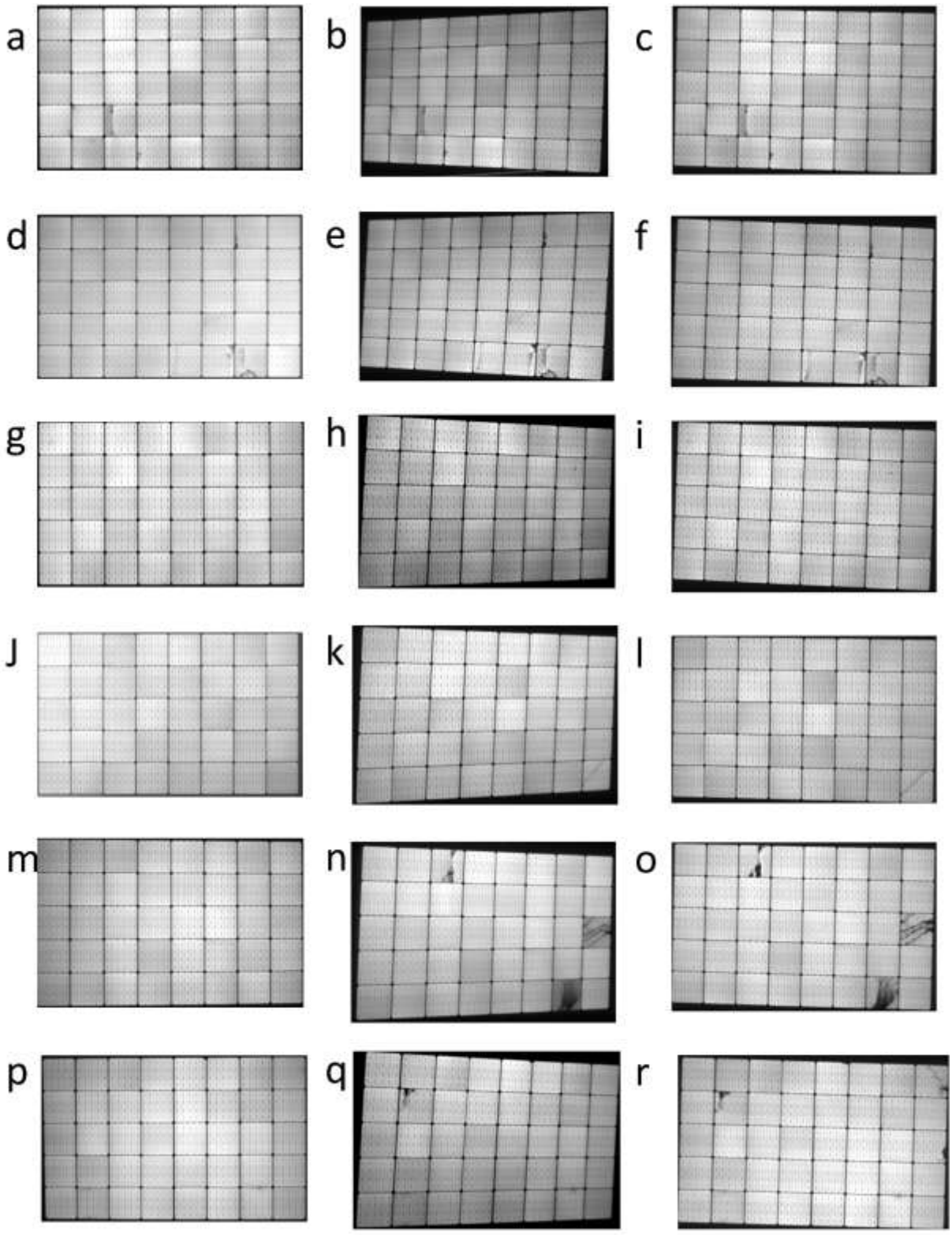

Fig. 41: EL images for modules mounted in the form of façade: PPGF6-Beige (a) in pristine condition, (b) after 3 months outdoor exposure, (c) after 9 months outdoor exposure; PPGF6-White (d) in pristine condition, (e) after 3 months outdoor exposure, (f) after 9 months outdoor exposure; PPGF6 (g) in pristine condition, (h) after 3 months outdoor exposure, (i) after 9 months outdoor exposure; PPGF8 (j) in pristine condition, (k) after 3 months outdoor exposure, (l) after 9 months outdoor exposure; PPGF8-White (m) in pristine condition, (n) after 3 months outdoor

exposure, (o) after 9 months outdoor exposure; PPGF8-Beige (p) in pristine condition, (q) after 3 months outdoor exposure, (r) after 9 months outdoor exposure

Table 12: IV characteristics for all the modules installed in the form of facade

Module	Condition	I_{sc} (A)	V_{oc} (V)	P_{max} (W)	FF	R_{series} (Ω)
PPGF6-BEIGE	0M	5.13	26.34	110.94	0.81	0.4
	3M	5.12	26.26	109.37	0.81	0.41
	9M	5.13	26.31	109.61	0.81	0.42
	Rel. % Change			**-1.21**		
PPGF6-WHITE	0M	6.24	26.51	134.08	0.8	0.37
	3M	6.3	26.5	133.29	0.8	0.37
	9M	6.28	26.47	133.28	0.8	0.38
	Rel. % Change			**-0.60**		
PPGF6	0M	9.06	26.91	193.61	0.79	0.32
	3M	9.09	26.86	191.79	0.79	0.31
	9M	9.1	26.83	191.14	0.78	0.32
	Rel. % Change			**-1.29**		
PPGF8	0M	9.25	26.92	195.74	0.8	0.29
	3M	9.26	26.84	194.91	0.78	0.3
	9M	9.17	26.84	193.89	0.79	0.31
	Rel. % Change			**-0.95**		
PPGF8-WHITE	0M	6.33	26.52	136.18	0.81	0.36
	3M	6.35	26.35	132.69	0.79	0.37
	9M	6.36	26.48	133.52	0.79	0.37
	Rel. % Change			**-1.99**		
PPGF8-BEIGE	0M	5.16	26.32	110.86	0.82	0.41
	3M	5.17	26.32	110.76	0.81	0.41
	9M	5.2	26.29	110.61	0.81	0.41
	Rel. % Change			**-0.22**		

2.6. Development of frameless module design with thin front glass and transparent backsheet at Kalyon PV, Turkey

2.6.1. Bill of materials

Thermoplastic polyolefin (TPO) encapsulants are classified into two types: crosslinking and non-crosslinking. The non-crosslinking TPO is an innovative encapsulant material that does not require peroxide crosslinking agents to maintain strong and stable laminates during the photo-voltaic module lamination process. As a result, it has zero gel content. This characteristic allows

non-crosslinking TPO to bypass the negative effects linked to peroxide-initiated crosslinking, positioning it as a viable alternative to traditional encapsulants like EVA, POE. Unlike EVA, whose properties dramatically change during curing, the physical properties of non-crosslinking TPO remain stable during lamination. TPO encapsulant is simply melted and simultaneously pressure applied to make intimate contact with the module components. Owing to thermoplastic nature, TPO encapsulants usually process at lower lamination pressure (600-800 mbar). Application of higher pressure will cause material flow out from edges and resulting in easy delamination or lower adhesion along the edges.

Two different coloured TPO polymeric films (light green and red terracotta) were sandwiched inside monocrystalline silicon modules, as a quasi-drop in the fabrication process of solar modules to produce the desired coloured appearance. The mini modules were fabricated in the structure of glass/ light green TPO/M10 PERC cells/ black TPO/backsheet and, glass/ red terracotta TPO/M10 PERC cells/ black TPO/backsheet respectively (Fig. 42 and Fig. 43). The most suitable selected lamination recipe information is given in Table 13.

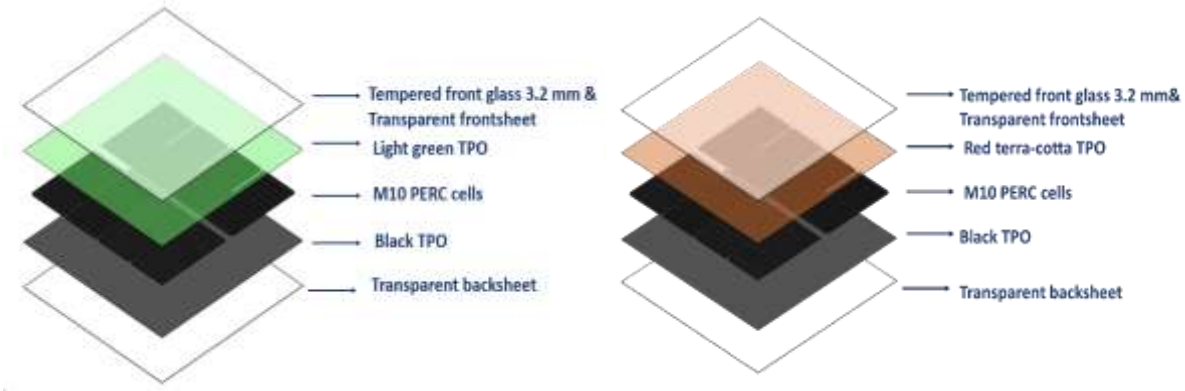

Fig. 42: Schematic representation of coloured mini modules

Table 13: Selected lamination recipe for coloured mini modules

T set up	145 °C
Pressure	80 kPa
Pumping Vacuum	200 s
Lamination	350 s
Inflate Time Indication	30 s

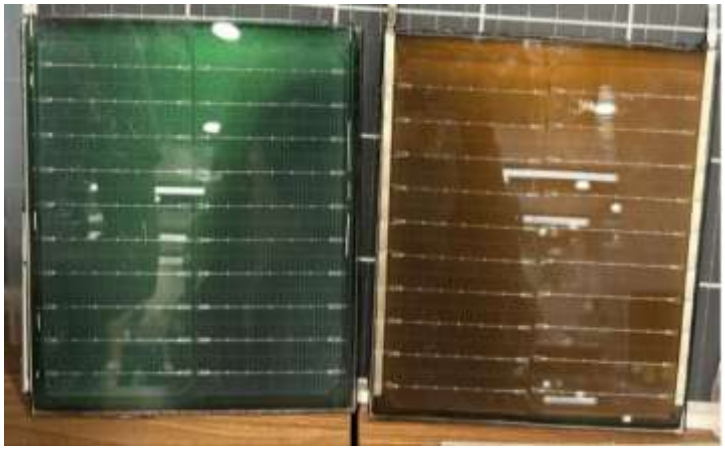

Fig. 43: Coloured PV mini modules produced at lab scale

Within the scope of the method development process, mini module production was initially carried out at the R&D level on a lab scale. The IV characterization of the produced mini modules was conducted. The electrical properties of the produced modules were investigated by means of current-voltage (I-V) characteristics measurements under standard test conditions. The application of two different colours polymeric encapsulants on the front side with the same amount of colour coverage implicates different electrical behaviour of the fabricated modules. The average efficiency of light green TPO based mini modules was found as 17.74% and the average efficiency of red terracotta TPO based mini modules was calculated as 16.95%. Current-voltage graph of coloured mini modules is shown in Fig. 44, below. The results are as follows (**Table 14**):

Table 14: IV results for coloured mini modules

Parameters	light green TPO based mini modules	red terracotta TPO based mini modules
Pmax (W)	23.51	22.45
Voc (V)	5.38	5.37
Isc (A)	5.51	5.28
Vpm (V)	4.46	4.45
Ipm (I)	5.27	5.04
FF	0.79	0.79
Eff (%)	17.74	16.95

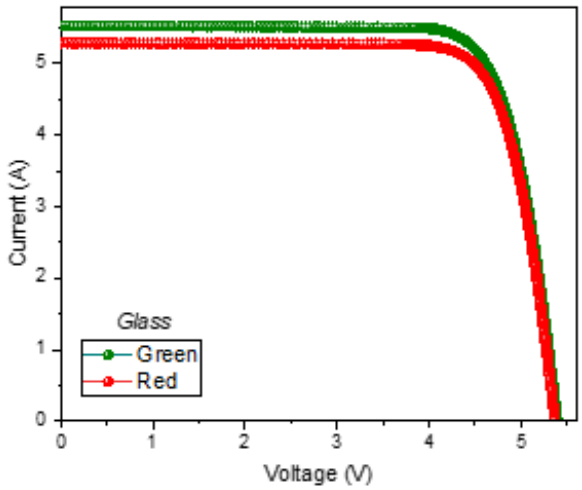

Fig. 44: I-V graph of coloured mini modules

A standard module production process contains several steps including front glass loading, encapsulant cutting and placement, stringing, module lay-up, auto bussing, back glass loading, edge sealing, lamination, attachment of the junction box, curing and power measurement. Amongst all process steps, stringing of cells and lamination steps are the most vital steps. In T2.4 Kalyon PV developed industrial processes for the fabrication of full size colored encapsulant based PV modules.

In the KalyonPV module line, 72 half-cut bifacial mono PERC full square solar cell based solar modules with colored encapsulant layers were fabricated with the proper lamination parameters Fig. 45. The electrical properties of the modules were investigated with solar simulator under AM1.5 G standard conditions at 25°C and 1000 W/m² illumination. The full-size PV modules were manufactured in the glass/glass structure. As Kalyon, customized industrial processes have been developed to produce products for BIPV applications using technologies and module components. Coloured module production has been carried out at production scale. IV characterization results of full-size coloured PV module are given below Table 15. Electroluminescence image results of the large size coloured PV module in Fig. 46, below.

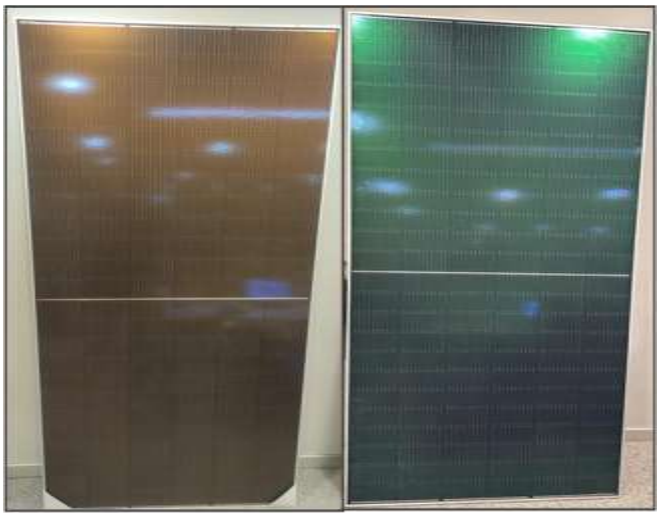

Fig. 45: Coloured modules produced in production scale

Table 15: Electrical parameters of fabricated PV modules on IV characterization tester in factory

Type	Pmax	Voc	Isc	Vpmax	ImA	Power	Current	Grade
standard	545.2	49.7	13.8	41.4	13.2	545	β	A
Colored encapsulanted module; (Light Green)	506.8	49.5	12.7	41.8	12.1	505	α	A
Colored encapsulanted module; (Terra Cotta)	471.6	49.2	11.9	41.5	11.3	470	α	A

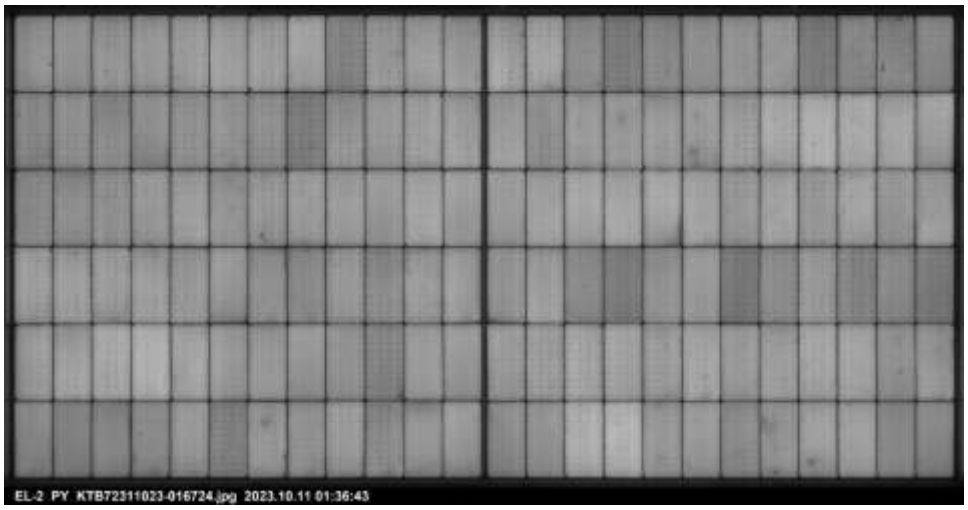

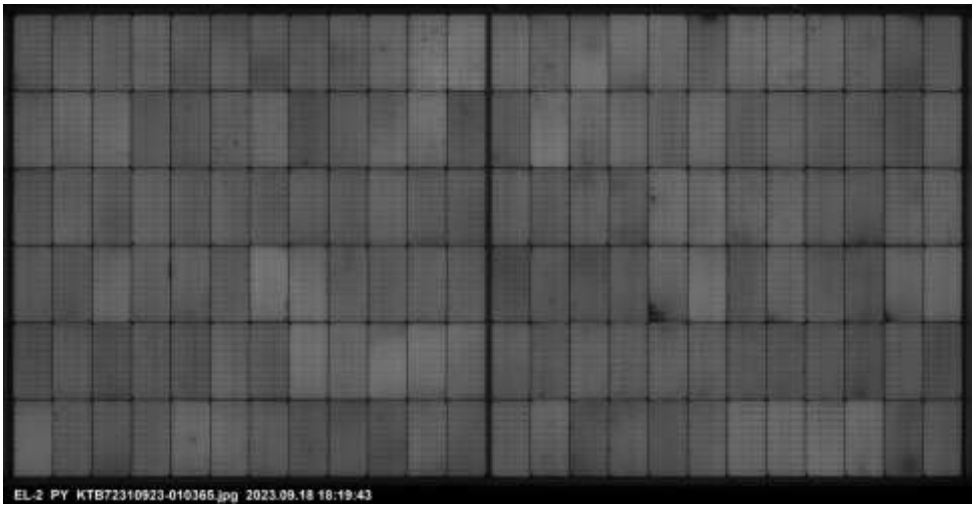

Fig. 46: Electroluminescence images for Coloured encapsulant based modules: Top: Terracotta; Bottom: Light Green

The produced coloured modules were sent to the outdoor test center of Kalyon and started to be subjected to a 1-year IV test there. In Fig. 47**Error! Reference source not found.**, an image is given from the outdoor test center for the one-year IV characterization monitoring service of the large-scale coloured modules produced. In addition to this, the first monthly electrical characterization results for coloured PV modules are given in the Table 16 below. Electroluminescence image results of the large size coloured PV module on outdoor test center are given in Fig. 48, below.

Fig. 47: Real image from the outdoor test center for the one-year I-V characterization monitoring service of the large-scale coloured modules produced.

Table 16: Electrical parameters of fabricated PV modules on IV characterization tester in outdoor test center

Type of Module	Encapsulant	Voc (V)	Isc (A)	Vm (V)	Im (A)	Power (W)	Eff loss (%)
Standard module	POE	49.9	13.7	41.8	13.1	544.5	-
Coloured encapsulanted module	Light Green TPO	49.8	12.3	41.7	12.9	511.9	5.9
Coloured encapsulanted module	Terra Cotta TPO	49.9	12.2	41.6	11.5	478.1	12.2

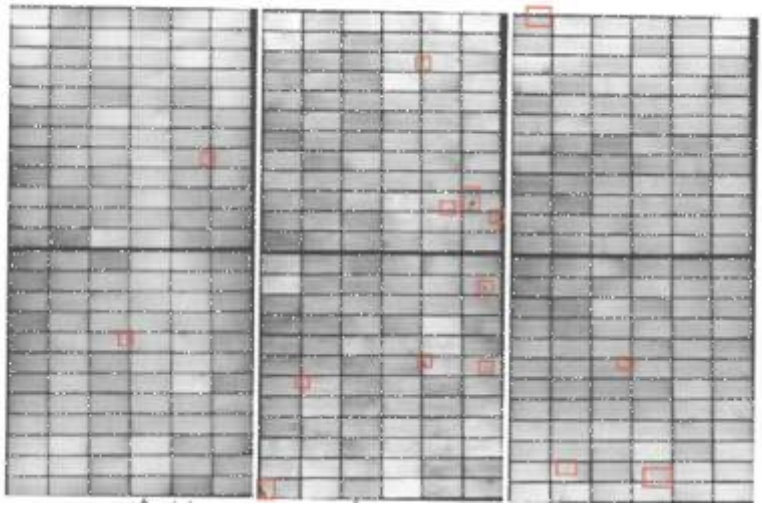

Fig. 48: Electroluminescence images results for coloured encapsulant based module on outdoor test center (left: standard, middle: terra cotta, right: light green)

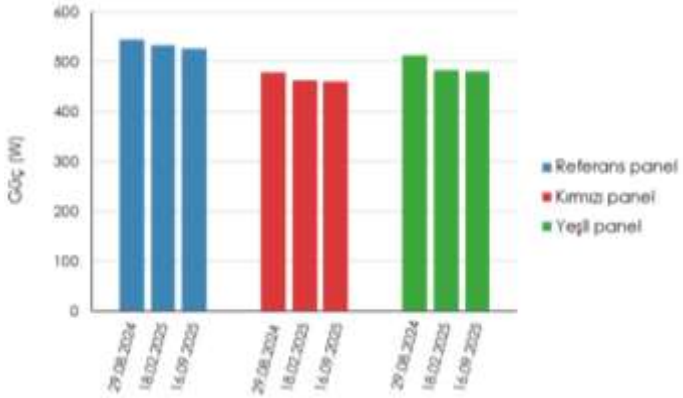

Fig. 49: power output in the STC condition for the three types of modules subjected to outdoor exposure for one year

As can be seen in Fig. 49, after 12 months of outdoor monitoring, the standard, terracotta, and green panels showed 3.31%, 3.55%, and 5.86% reduction in power output, respectively. Performance ratio values were recorded to be 93.0% (standard), 85.5% (terracotta), and 84.9% (green).

3 Conclusions and outlook

This report presents the outcomes of developing lightweight, aesthetically pleasing PV modules for building integration. The two main types of module design targeted in this work are: glass free design to achieve ≤6 kg/m² weight and design with front glass to achieve ≤7 kg/m² for frameless full-size lightweight modules. Furthermore, it also discussed main results on the innovative frontsheet coatings developed for protection of modules from environmental stressors. The work extensively focused on assessing the reliability of the novel module architectures against environmental stressors, mechanical loads and also assessed fire safety. Finally, outdoor testing for about a year in two countries situated in two different climatic conditions, i.e., Switzerland and Turkey are also performed and reported. Important conclusions of the project as listed below:

- The modules based on the novel composite backsheets could achieve the target of weight less than **6 kg/m²**.
- PET-based skin-HC combinations were not found suitable for use in the form of PV modules. **PP-based skin-HC combinations were deemed suitable in the initial round of testing and were selected for further improvement and testing**.
- A bill-of-materials for LW PV modules, that can pass the qualification criteria as per IEC 61215, is identified as a PET-based frontsheet, polyolefin elastomer (POE) as an encapsulant, Solaxess colored polymer foils for aesthetical improvements, PERC cells, and PP-based HC-skin backsheet. The two composite backsheet candidates (PPGF6 and PPGF8) consisted of the same PP-based honeycomb but were different in the skins. The first candidate, PPGF8, had white skin with 820 g/m² fiber density, while the second, PPGF6 is black with 660 g/m² fiber density.
- Accelerated sequential tests comprising combination of various stressors such as, thermal cycling, UV irradiance, damp-heat, humidity freeze cycling, mechanical loads and hail impact tests were performed on the modules of larger format. The modules passed the three different sequences and showed power output degradation less than 5 % (relative)—thus passing the criteria.
- The flammability tests conducted on the minimodules showed to have passed ISO Class E; however, flaming droplets were observed in both cases, preventing full Class E compliance.
- A test demo site has been created on the rooftop of microcity building at Neuchâtel, Switzerland. Where all the LW module candidates are attached in the form of an East-facing façade for monitoring in the MPP tracking mode. It is found that for some of the modules, new cracks appear close to the corner of the modules—indicating the module design sensitive to mounting induced stresses. Furthermore, for an intact module based on PPGF6, after 9 months of outdoor exposure, the power out put degraded by about 1.29 %.

- Among the novel frontsheet coating solutions, monomer A is identified as better candidate than monomer B to provide better protection against both UV and DH ageing when laminated in the form of a mini-module.
- For the module design based on glass/transparent backsheet architecture, the power out put after one year outdoor exposure was found to be 3.31%, 3.55%, and 5.86% for the standard, terracotta, and green modules, respectively.

Overall, this work demonstrates promising outcomes for the novel module architectures, especially for the glass-free design. Under the accelerated conditions the modules not only passed the requirements but exceeded them and later when subjected to outdoor conditions for about 9 months, do not show significant degradation. Mini-modules pass the standards that make the installation suitable for buildings of height less than 11 m. It is noted that adding fire retardants at the level of encapsulants and backsheets may further enhance the safety of these modules.

4 Publications and other communications

Type	Description	Year
Journal paper	*Umang Desai, Marie Courtant, Gabriele Eder, Gernot Oreski, Antonin Faes, Christophe Ballif, "* ***Novel mechanically robust and environmentally stable light-weight colored photovoltaic modules based on composite polymer backsheets****"*	*2025, Solar RRL, 9 (12). http://doi.org/10.1002/solr.202500177*
Poster	*Umang Desai, Leïla Mazirt, Yuliya Voronko, Gabriele Eder, Nikolina Pervan, Gernot Oreski, Antonin Faes, Christophe Ballif, "****Façade Application of Light-Weight Glass-Free Colored PV Modules: Reliability Testing of the Large-Format Modules and Monitoring of the Demonstration Site****"*	42nd European Photovoltaic Solar Energy Conference and Exhibition, 2025, Bilbao, Spain
Journal paper	*Nikolina Pervan, Umang Desai, Gabriele C Eder, Jonathan Govaerts, Arne Derluyn, Wouter Winant, Antonin Faes, Christophe Ballif, Gernot Oreski, "****Characterization of Lightweight Polymeric Honeycomb Structures for Use as Backsides in Glass-Free PV Modules****"*	2025, Journal of Applied Polymer Science.
Poster	*Nikolina Pervan, Gabriele C. Eder, Yuliya Voronko, Umang Desai, Antonin Faes, Christophe Ballif, Jarne Saelens, Wouter Winant, Bin Luo, Jonathan Govaerts, Gernot Oreski,* ***"Honeycomb structures as backsheets for light weight PV modules"***	PV in Motion Conference, 06. - 08. 03. 2024. Neuchatel (CH)
Presentation	*Umang Desai, Jonathan Govaerts, Bin Luo, Yuliya Voronko, Gabriele Eder, Jarne Saelens, Wouter Winant, Nikolina Pervan, Gernot Oreski, Antonin Faes, Christophe Ballif,* ***"Novel lightweight PV modules based on polymeric honeycomb for building integration"***	IEEE-PVSC, 9.-14.06.2024, Seattle (USA)
Poster	*Nikolina Pervan, Sonja Feldbacher, Gabriele C. Eder, Yuliya Voronko, Umang Desai, Antonin Faes, Christophe Ballif, Wouter Winant, Bin Luo, Jonathan Govaerts, Gernot Oreski, "****Enabling glass-free light weight PV modules via honeycomb structures"***	EUROREG Conference, 20. – 21. 06. 2024., Ljubljana (SI)

Presentation	*Umang Desai, Jonathan Govaerts, Bin Luo, Yuliya Voronko, Gabriele Eder, Jarne Saelens, Wouter Winant, Nikolina Pervan, Gernot Oreski, Antonin Faes, Christophe Ballif,* ***"Mechanically Robust and Environmentally Stable Novel Lightweight PV Modules for Building Integration Based on Polymeric Honeycomb"***	41st European Photovoltaic Solar Energy Conference and Exhibition, 23.-27.9.2024, Vienna (AUT)
Poster	*Leïla Mazirt, Umang Desai, Yuliya Voronko, Nikolina Pervan, Gernot Oreski, Gabriele Eder, Antonin Faes, Christophe Ballif,* ***"Upscaling of lightweight polymeric honeycomb based solar panels for BIPV"***	Solar and Storage conference, 17-18 09.2024, Zürich (CH)
Invited talk	*U. Desai, F. Lisco, A. Virtuani, A. Faes, C. Ballif,* ***Development and testing of light weight PV modules***	SOPHIA PV Module Reliability Workshop, Italy, 2023
Presentation	*Jonathan Govaerts, Paul Dufke, Bin Luo, Matthias Bonnart, Rik Van Dyck, Tom Borgers, Jef Poortmans, Arne Derluyn, Jarne Saelens, Wouter Winant, Meric Caliskan, Arslan, Umang Desai, Fabiana Lisco, Antonin Faes, Christophe Ballif, Gernot Oreski, Nikolina Pervan, Gabriele Eder,* ***Light as heaven, strong as hell(?): Testing honeycomb-based laminates for light-weight c-si PV applications***	*EU PVSEC, Portugal, 2023*
Poster	*U. Desai et al,* ***Overview of the project "DELIGHT" DE sign and Evaluation of LIGHT weight Composite PV Modules for Integration in Buildings and Infrastructure***	*21st Swiss Solar Conference, Bern, 2023*
Poster	*N. Pervan et al.,* ***Honeycomb structures as backsheets for light weight PV modules***	*EU PVSEC, Portugal, 2023*